iScience

CellPress
OPEN ACCESS

Article

High-throughput longitudinal electrophysiology screening of mature chamber-specific hiPSC-CMs using optical mapping

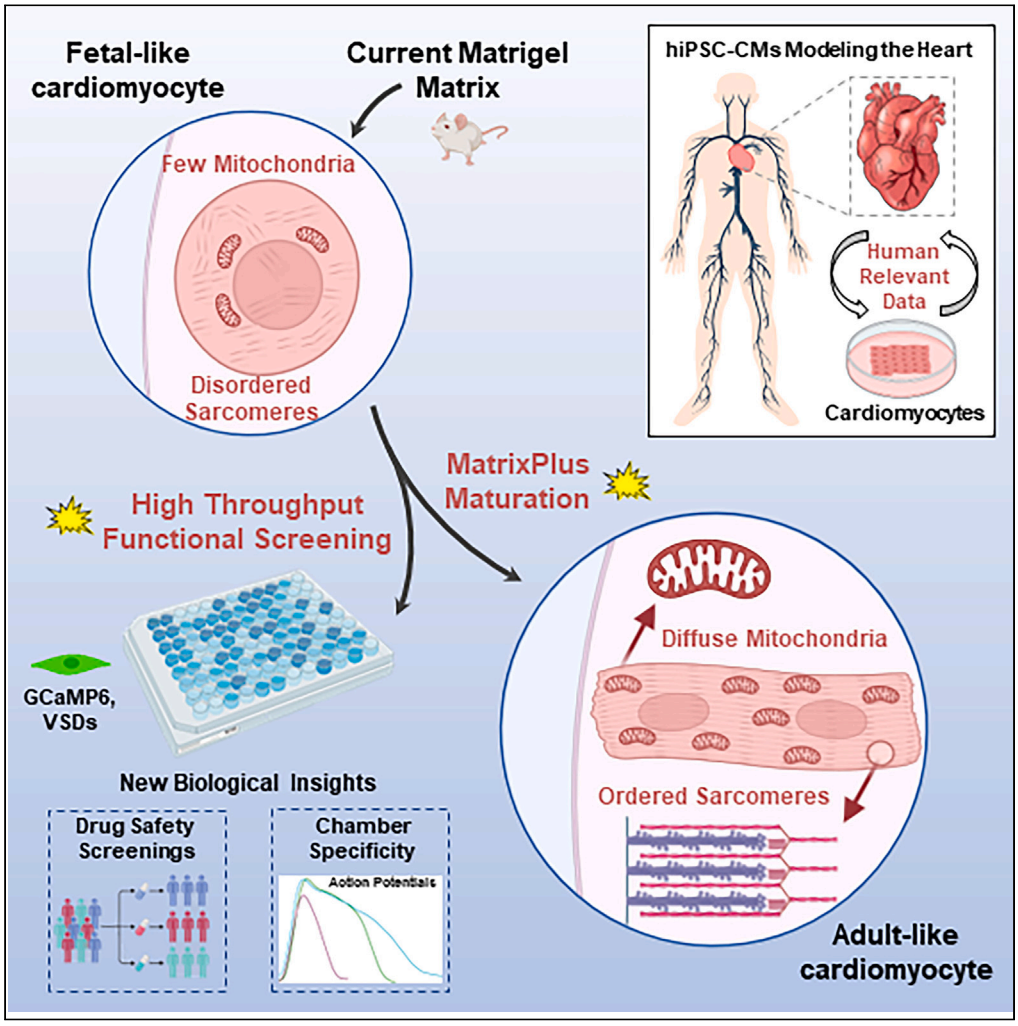

Andrew Allan, Jeffery Creech, Christian Hausner, ..., Andre Monteiro da Rocha, Deok-Ho Kim, Todd J. Herron

toddherr@umich.edu

Highlights

A method for high-throughput maturation of hiPSC-CMs via human extracellular matrix

Rapidly mature hiPSC-CMs in 2D cell culture plates in just 7 days

High-throughput cardiac electrophysiology screening using fluorescent dyes

Longitudinal measures of hiPSC-CM calcium flux using GECI-GCaMP6

Allan et al., iScience 26, 107142
July 21, 2023
https://doi.org/10.1016/j.isci.2023.107142

iScience

CellPress
OPEN ACCESS

Article

High-throughput longitudinal electrophysiology screening of mature chamber-specific hiPSC-CMs using optical mapping

Andrew Allan,[1] Jeffery Creech,[2] Christian Hausner,[2] Peyton Krajcarski,[2] Bianca Gunawan,[2] Noah Poulin,[2] Paul Kozlowski,[3] Christopher Wayne Clark,[4] Rachel Dow,[2] Prakaimuk Saraithong,[2,3] Devin B. Mair,[5] Travis Block,[6] Andre Monteiro da Rocha,[2,3] Deok-Ho Kim,[5] and Todd J. Herron[2,3,7,8,*]

SUMMARY

hiPSC-CMs are being considered by the Food and Drug Administration and other regulatory agencies for *in vitro* cardiotoxicity screening to provide human-relevant safety data. Widespread adoption of hiPSC-CMs in regulatory and academic science is limited by the immature, fetal-like phenotype of the cells. Here, to advance the maturation state of hiPSC-CMs, we developed and validated a human perinatal stem cell-derived extracellular matrix coating applied to high-throughput cell culture plates. We also present and validate a cardiac optical mapping device designed for high-throughput functional assessment of mature hiPSC-CM action potentials using voltage-sensitive dye and calcium transients using calcium-sensitive dyes or genetically encoded calcium indicators (GECI, GCaMP6). We utilize the optical mapping device to provide new biological insight into mature chamber-specific hiPSC-CMs, responsiveness to cardioactive drugs, the effect of GCaMP6 genetic variants on electrophysiological function, and the effect of daily β-receptor stimulation on hiPSC-CM monolayer function and SERCA2a expression.

INTRODUCTION

In 2009 Zhang et al.[1] reported that hiPSCs (human induced pluripotent stem cells) can generate functional cardiomyocytes as well as hESCs (human embryonic stem cells) and thus offer an alternative source for human cardiomyocyte production.[2–4] In fact, the use of hiPSC-CMs is becoming widespread for regulatory science,[5–7] cardiovascular disease modeling,[8–11] and development of regenerative therapies.[12,13] Furthermore, owing to the patient-specific nature of using hiPSC-CMs, *in vitro* "Clinical Trials in a Dish" are being considered for regulatory science in order to increase representation of diverse population demographics, ensure safety of medications for all patients, and reduce the cost of drug development.[14,15] hiPSC-CMs are available from commercial sources as cryopreserved vials of ready-to-use cells[16] or can be generated in the laboratory using hiPSCs and cardiac-directed differentiation approaches.[17,18] For regulatory science and cardiotoxicity screening, commercially available hiPSC-CMs have been validated in blinded multi international site studies.[6,14,19] Despite the utility and promise of hiPSC-CM *in vitro* assays to replace current regulatory guidelines, there are technical and cellular advances required for widespread adoption.

The typical phenotype of hiPSC-CMs is characterized by fetal-like structure and function, but recent developments in 2D extracellular matrix (ECM) engineering have improved the maturation of hiPSC-CMs (as well as hESC-CMs) to resemble adult cardiomyocytes.[18,20–23] Using the optimal ECM it is possible now to significantly mature the structural and functional phenotypes of 2D hiPSC-CMs in as few as seven days.[18,20] Seven-day maturation is a major advance over previous approaches requiring over 100 days for modest maturation.[24–26] This is critical for using hiPSC-CMs in pre-clinical drug safety screening because the maturation state of hiPSC-CMs is known to impact drug responsiveness.[20,27] Although 3D cell culture approaches have demonstrated hiPSC-CM maturation,[28–30] these approaches require complex chronic electrical pacing (up to 28 days) and mixture of heterologous proliferative cells with hiPSC-CMs in low-throughput systems. 2D monolayers provide a more reproducible and defined cell system using purified cardiomyocytes with greater efficiency and economical use of cardiomyocyte use for *in vitro* studies. Still,

[1]Cairn Research, Graveney Road, Faversham, Kent ME13 8UP UK

[2]University of Michigan, Frankel Cardiovascular Regeneration Core Laboratory, Ann Arbor, MI 48109, USA

[3]Michigan Medicine, Internal Medicine-Cardiology, Ann Arbor, MI 48109, USA

[4]University of Michigan, School of Public Health, Department of Environmental Health Sciences, Ann Arbor, MI 48109, USA

[5]Department of Biomedical Engineering, The Johns Hopkins University School of Medicine, Baltimore, MD 21205, USA

[6]StemBioSys, Inc, 3463 Magic Drive, Suite 110, San Antonio, TX 78229, USA

[7]Michigan Medicine, Molecular & Integrative Physiology, Ann Arbor, MI 48109, USA

[8]Lead contact

*Correspondence: toddherr@umich.edu

https://doi.org/10.1016/j.isci.2023.107142

widespread adoption of hiPSC-CM *in vitro* assays to replace the existing testing paradigm requires high-throughput maturation combined with high-throughput screening of electrophysiological function. Here we utilize human ECM pre-coated 96-well plates to mature hiPSC-CM phenotypes in a robust way using multiple hiPSC lines. Importantly, we validate this maturation approach using both cryopreserved commercially available hiPSC-CMs and in-house generated hiPSC-CMs.

Cardiac optical mapping using voltage-sensitive dyes (VSDs), calcium-sensitive dyes, or genetically encoded calcium indicators (GECIs) offers an hiPSC-CM *in vitro* assay with high spatiotemporal resolution.[31] In fact, a recent "Best Practices" paper on the use of hiPSC-CMs for pre-clinical cardiotoxicity ranked cardiac optical mapping over multi-electrode array (MEA) assays for providing granularity to predicting proarrhythmia and cardiotoxicity.[32] Here we designed and validated a cardiac electrophysiology plate reader for high-resolution and high-throughput assessment of hiPSC-CM electrophysiology using VSDs, calcium-sensitive probes, and GECI. Instrument validation was performed using medications with known cardioactive effects to confirm cardiac chamber-specific (atrial or ventricular) differentiation of hiPSCs. We also use this instrument to provide important new biological insight into the effects of GCaMP6 variants (fast, medium, or slow calcium binding) on hiPSC-CM function and utility for optically based repeated measures. GCaMP6 expression-enabled repeated measures of spontaneous calcium flux were utilized to confirm daily β-adrenergic receptor stimulation of hiPSC-CM monolayers. This robust maturation approach using 2D hiPSC-CM monolayers together with high-throughput electrophysiology screening will hasten widespread adoption of these human-based assays and promote the 3Rs of animal usage in research: replacement, reduction, and refinement.[33]

RESULTS

Human perinatal stem cell-derived ECM coating and maturation of hiPSC-CMs

In 2020 we reported the discovery of a perinatal stem cell-derived ECM that promoted the maturation of hiPSC-CMs.[20] Here the ECM-coated plates are manufactured using automation for large-scale production. This ECM is available commercially under the product name CELLvo MatrixPlus (StemBioSys, Inc.). Briefly, immortalized amniotic fluid stem cells are seeded onto fibronectin-coated cultureware and cultured to confluence prior to being induced by increasing the concentration of ascorbic acid in the media to secrete matrix. The resulting matrix is decellularized using non-ionizing detergent, washed thoroughly, and allowed to airdry for long-term storage. Prior to use, the dried and decellularized matrix is rehydrated by incubation with PBS.

hiPSC-CM cell shape and mitochondrial function were measured using confocal imaging and staining with JC-1 dye for mitochondrial membrane potential quantification (Figures 1A, 1B, and S1). hiPSC-CM mitochondrial membrane potential is significantly depolarized in the immature CMs plated on Matrigel-mouse ECM compared to mature CMs plated on MatrixPlus-human ECM (Figure 1B). Immunofluorescent staining of hiPSC-CMs plated on a commonly used ECM (Matrigel-mouse ECM) or on MatrixPlus-human ECM further reveals the maturation-inducing effects (Figure 1C). Immunostaining for the sarcomere protein, α-actinin (red), indicates immature hiPSC-CMs maintained on Matrigel with characteristic fetal-like appearance of circular cells and disorganized radially oriented sarcomere pattern. On the other hand, hiPSC-CMs plated on MatrixPlus-human ECM are rod shaped and express highly organized sarcomeres, with a greater average sarcomere length of 1.86μm compared to immature hiPSC-CMs plated on Matrigel-mouse ECM (1.61 μm, Figure 1D). Phase-contrast and whole-cell fluorescent images were used to calculate the circularity index of hiPSC-CMs from multiple hiPSC sources (Figures 1E and 1F). MatrixPlus ECM promotes rod-shaped morphology of hiPSC-CMs from four different cell lines (Figures 1F and S2–S4). Regardless of the imaging approach used for phenotype analysis or the hiPSC line used, hiPSC-CMs cultured on MatrixPlus-human ECM consistently present a rod-shape morphology, like adult mammalian cardiomyocytes. Finally, electrical impulse propagation velocity was faster in hiPSC-CM monolayers plated on MatrixPlus ECM compared to those plated on Matrigel-mouse ECM (Figure 1G; iPS PENN002i-442-1 atrial cardiomyocytes).

Cardiac EP plate reader: Design and functional validation using medications with known cardioactive effects

For high-throughput data collection, we designed and built a cardiac EP plate reader (Figure S5). The cardiac EP plate reader enabled high-throughput functional screening using mature hiPSC-CMs in 96-well plate format (Video S1). Analysis software was also created for parallel processing of all 96 wells and

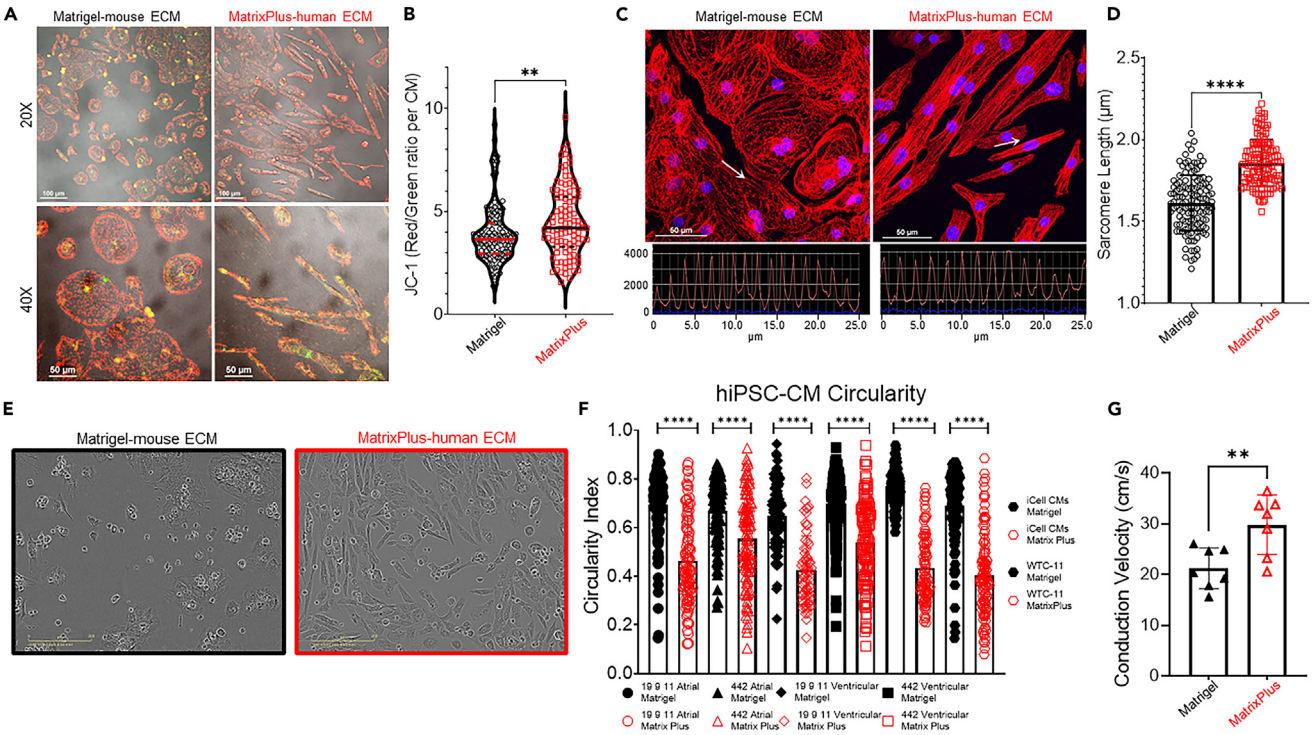

Figure 1. MatrixPlus-human ECM promotes maturation of hiPSC-CM structure and mitochondrial function

(A) hiPSC-CM mitochondrial function was measured using JC-1 mitochondrial-specific fluorescent marker.

(B) JC-1 red-to-green ratio was greater in hiPSC-CMs plated on MatrixPlus-human ECM (4.51 ± 1.69 fluorescence units, n = 102 hiPSC-CMs) than hiPSC-CMs plated on Matrigel-mouse ECM (3.90 ± 1.43 fluorescence units, n = 114 hiPSC-CMs). **p = 0.0046, unpaired t test.

(C) Sarcomere staining using α-actinin-specific antibody and confocal imaging shows distinct sarcomere organization between hiPSC-CMs plated on Matrigel-mouse ECM and MatrixPlus-human ECM. The white arrow in each picture was used to make the intensity profile plots for α-actinin periodicity over 25μm.

(D) hiPSC-CMs maintained on Matrigel-mouse ECM have significantly shorter sarcomere length (1.61 ± 0.17μm, n = 129) than hiPSC-CMs maintained on MatrixPlus-human ECM (1.86 ± 0.14μm, n = 129). ****p < 0.0001, unpaired t test.

(E) Live cell phase-contrast images (20X) show the difference of shape between hiPSC-CMs maintained on Matrigel-mouse ECM compared to the same batch of hiPSC-CMs maintained on MatrixPlus-human ECM.

(F) hiPSC-CM circularity index was quantified using multiple hiPSC lines with chamber specification or without chamber specification. For each cell line, black symbols represent the cell circularity on Matrigel-mouse ECM while red symbols represent the cell circularity on MatrixPlus-human ECM. Statistical comparisons were made within each group plated on each ECM. ****p < 0.0001, unpaired t tests, n = 77–109 hiPSC-CMs per group.

(G) Optical mapping calcium transient wave conduction was faster in hiPSC-CM monolayers maintained on MatrixPlus-human ECM (Matrigel = 21.2 ± 4.0 cm/s; n = 7 vs. MatrixPlus-human ECM = 29.8 ± 5.9 cm/s; n = 7. **p = 0.0078, unpaired t test. Data are expressed as mean ± standard deviation.

generation of whole-plate heatmaps for quantification of electrophysiological parameters (Figures S5 and S6). The cardiac EP plate reader was first validated using calcium- or voltage-specific fluorescent probes. VSDs and calcium-sensitive fluorophores enable direct measurement of hiPSC-CM action potentials (APs) or intracellular calcium transients (CaTs). To validate the cardiac EP plate reader, we measured atrial hiPSC-CM monolayer APs (FluoVolt) or CaT (CalBryte520AM) properties (Figure 2). Each parameter was measured from separate wells; half of the wells were loaded with FluoVolt, and the remaining wells of each plate were loaded with CalBryte520AM. First we compared VSD and CaT data to ensure the recapitulation of the well-known temporal relationship between APs and CaTs.[34] High-resolution atrial hiPSC-CM monolayer AP and CaT recordings typically recorded using the cardiac EP plate reader are presented in Figures 2A and 2B. Spontaneous beat rate and impulse propagation velocity were similar regardless of parameter measured (Figures 2C and 2D). Notably, here the conduction velocity values (~50 cm/s) are near the values recorded in adult human hearts, indicating an advanced degree of hiPSC-CM functional maturation. This is a significant advance over MEA-based approaches where conduction velocity is much slower (10–20 cm/s) likely due to the immature phenotype of the hiPSC-CMs.[35,36] CaT duration 80 (CaTD80) was significantly longer than AP duration 80 (APD80, Figure 2E), and CaT triangulation was greater than AP triangulation (Figure 2F). Color-coded heatmaps for APD30, APD90, CaTD30, CaTD90, and triangulation show the expected temporal differences between the parameters (Figures 2G–2I).

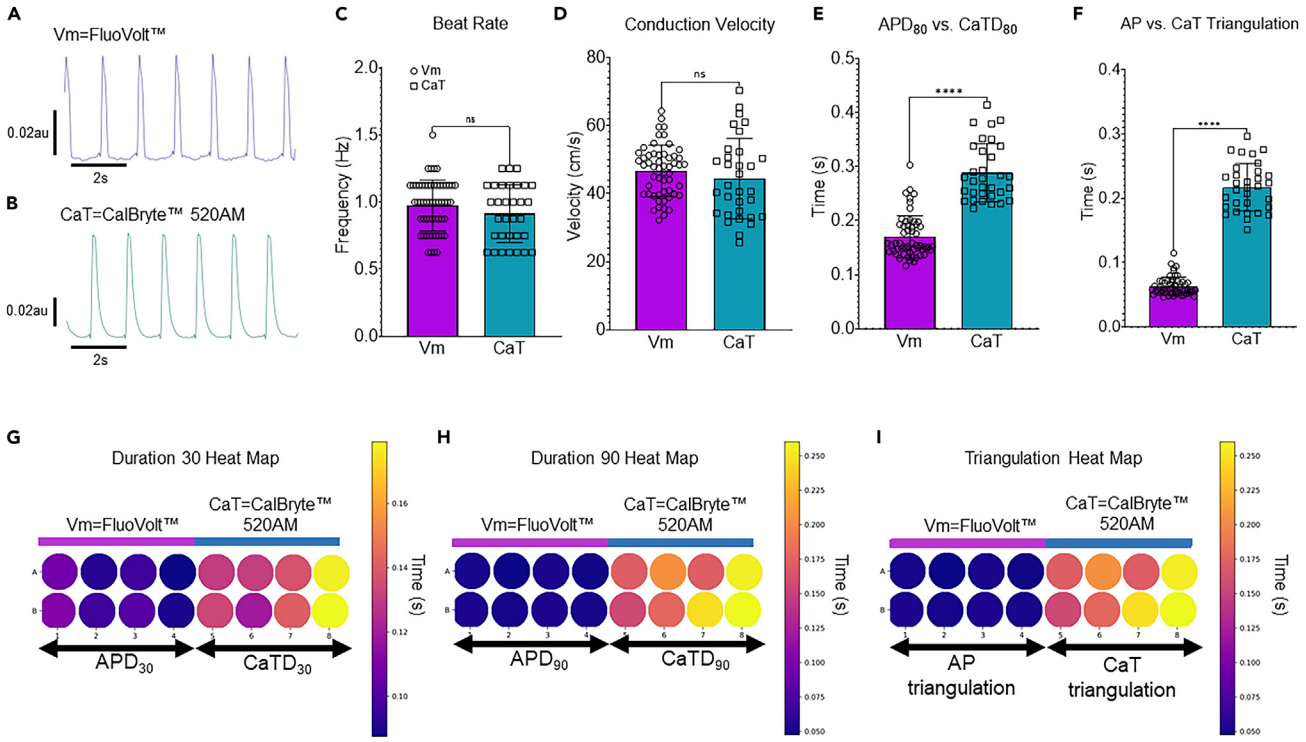

Figure 2. Validation of voltage-sensitive dye and calcium-sensitive dye high-throughput electrophysiology assays

(A) Representative recording of atrial hiPSC-CM monolayer action potentials using FluoVolt.

(B) Representative recording of atrial hiPSC-CM monolayer calcium transients using CalBryte 520AM.

(C) The spontaneous beat rate of atrial hiPSC-CM monolayers was similar regardless of parameter measured (Vm = 0.98 ± 0.19 Hz, n = 56 monolayers; CaT = 0.91 ± 0.21 Hz, n = 32 monolayers; unpaired t test, ns). This represents 56 and 32 technical monolayer replicates, respectively.

(D) Impulse conduction velocity was similar between each parameter measured (Vm = 46.7 ± 7.5 cm s-1, n = 55 monolayers; CaT = 44.5 ± 11.8 cm s-1, n = 32 monolayers; unpaired t test, ns).

(E) APD80 was significantly shorter than CaTD80 (Vm = 0.170 ± 0.04 s, n = 56 monolayers; CaT = 0.289 ± 0.05 s, n = 32 monolayers technical replicates; unpaired t test, ****p < 0.0001).

(F) AP triangulation was significantly lower than CaT triangulation (Vm = 0.06 ± 0.01 s, n = 56 monolayers; CaT = 0.22 ± 0.04 s, n = 32 monolayers; unpaired t test, ****p < 0.0001).

(G) APD or CaT duration 30 heatmap for 8 representative wells per group.

(H) APD or CaT duration 90 heatmap for 8 representative wells per group.

(I) AP or CaT triangulation heatmap for 8 representative wells per group. Data are expressed as mean ± standard deviation.

Next, hiPSC-CM monolayer responsiveness to medications with known risk to cause arrhythmias was tested to further validate the cardiac EP plate reader assay (Figures 3, S7, andS8). Isoproterenol (ISO) is a non-specific β adrenoceptor agonist that stimulates positive inotropy and chronotropy in mature cardiac tissues and cells. Mobilization of intracellular calcium is the primary mechanism underlying the cardiomyocyte ISO response, so we measured CaTs (CalBryte520AM) to provide a more direct measure of this signaling cascade. Atrial hiPSC-CM monolayers response to ISO included increased spontaneous beat rate, increased impulse conduction velocity, and increased CaT amplitude (Figures 3A–3D). E−4031 is a hERG channel-specific blocker that, when applied to atrial hiPSC-CM monolayers, prolonged APD (Figure S7C). E−4031 also reduced impulse conduction velocity, reduced CaT amplitude, and dramatically prolonged the CaTD80 (Figures 3F–3J). Slowing of conduction velocity by E−4031 has been reported before[37] in canine hearts and is due to the depolarization of the CM resting membrane potential making fewer voltage-gated sodium channels available for activation and impulse conduction.[38] Ibutilide is a class III anti-arrhythmic drug used for acute cardioversion of atrial fibrillation and atrial flutter to sinus rhythm. Ibutilide acts by induction of slow inward sodium current which prolongs APD (in addition to hERG channel blocking effects) and refractory period of cardiomyocytes. Atrial hiPSC-CMs showed the expected response to a high dose of ibutilide (0.1μM), including slower conduction velocity, reduced contractility (reduced CaT amplitude), and prolongation of the CatD (Figures 3K–3O). Vandetanib is an anti-cancer therapy used to treat thyroid cancers and is classified with a high risk to cause fatal arrhythmias; here we

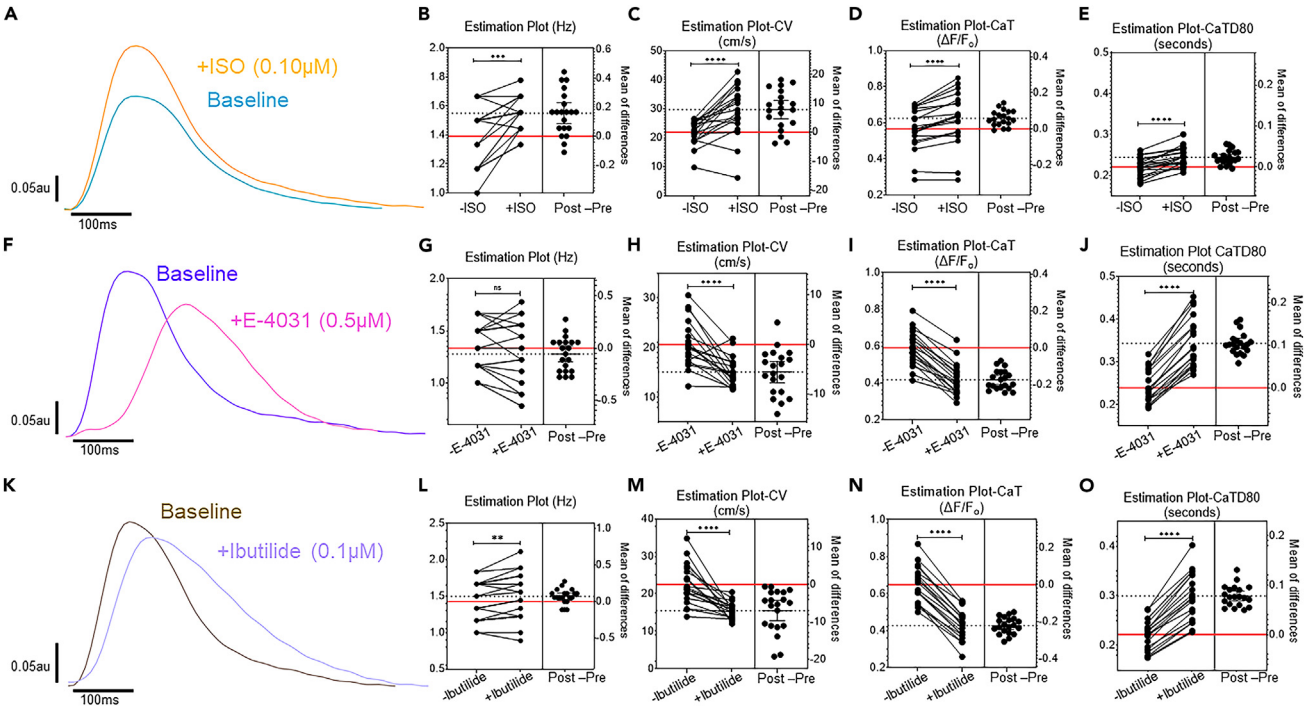

Figure 3. Cardiac optical mapping validation using three cardioactive compounds applied to atrial hiPSC-CM monolayers

(A) Representative before and after calcium transient traces of a single well treated with isoproterenol (+ISO, 0.10μM).

(B) Paired analysis indicates increased spontaneous beat rate after ISO treatment. (Paired t test, ***p = 0.002, n = 20 monolayer technical replicates).

(C) Impulse conduction velocity was increased following ISO treatment. (Paired t test, ****p < 0.0001, n = 20 monolayers).

(D) Calcium transient amplitude (ΔF/F0) was increased after ISO treatment. (Paired t test, ****p < 0.0001).

(E) CaTD80 was slightly greater following ISO treatment. (Paired t test p < 0.0001).

(F) Representative before and after calcium transient traces of a single monolayer treated with E−4031 (+E−4031, 0.5μM).

(G) Paired analysis indicates lack of effect of E−4031 on atrial hiPSC-CM monolayer beat rate.

(H) Conduction velocity was significantly slower with E−4031 treatment. (Paired t test, ****p < 0.0001, n = 20 monolayers).

(I) Calcium transient amplitude (ΔF/F0) was reduced by E−4031 treatment. (Paired t test, ****p < 0.0001).

(J) E−4031 significantly increased CaTD80. (Paired t test, ****p < 0.0001).

(K) Representative traces show the effect of Ibutilide (0.1μM) on the calcium transient.

(L) Ibutilide slightly increased the beat rate. (Paired t test, **p = 0.007).

(M) Ibutilide slowed conduction velocity. (Paired t test, ****p < 0.0001, n = 20 monolayer technical replicates).

(N) Ibutilide treatment reduced the calcium transient amplitude (ΔF/F0). (Paired t test, ****p < 0.0001).

(O) Ibutilide significantly increased CaTD80. (Paired t test, ****p < 0.0001). Data are expressed as mean ± standard deviation.

observed slowing of beat rate and prolongation of the CaT in response to this medication (Figure S7). Ranolazine is a heart medication used to treat angina and has very low risk to cause arrhythmias despite causing slight QT prolongation attributed to off-target effects blocking the hERG potassium channel. Here we tested the mature hiPSC-CM response to ranolazine using clinically relevant concentrations based on a recent Food and Drug Administration (FDA)-led validation study.[5,6] *In vitro* atrial hiPSC-CM beat rate and rhythm were undisturbed by ranolazine treatment (Figures S8A–S8E) at all doses, but AP prolongation (surrogate for QT prolongation) was observed at high doses of ranolazine. Domperidone is a medication used to treat nausea and vomiting often caused by other drugs to treat disease like Parkinson's. Domperidone can block the hERG ion channel and is labeled a medication with intermediate risk to cause fatal arrhythmias.[5,19] We tested the effect of domperidone on atrial hiPSC-CMs by measuring intracellular calcium flux response to clinically relevant doses (Figures S8F–S8J). The highest dose of domperidone reduced spontaneous beat rate, prolonged the CaTD80, and increased the CaT triangulation.

Cardiac chamber-specific hiPSC-CM functional validation using the cardiac EP plate reader

We generated chamber-specific hiPSC-CMs using an established protocol that characterized the molecular and functional phenotypes of atrial- and ventricular-specific CMs.[17] Here, the 19-9-11 control vector free hiPSC line (male) and PENN002i-442-1 control vector free hiPSC line (female) were used for

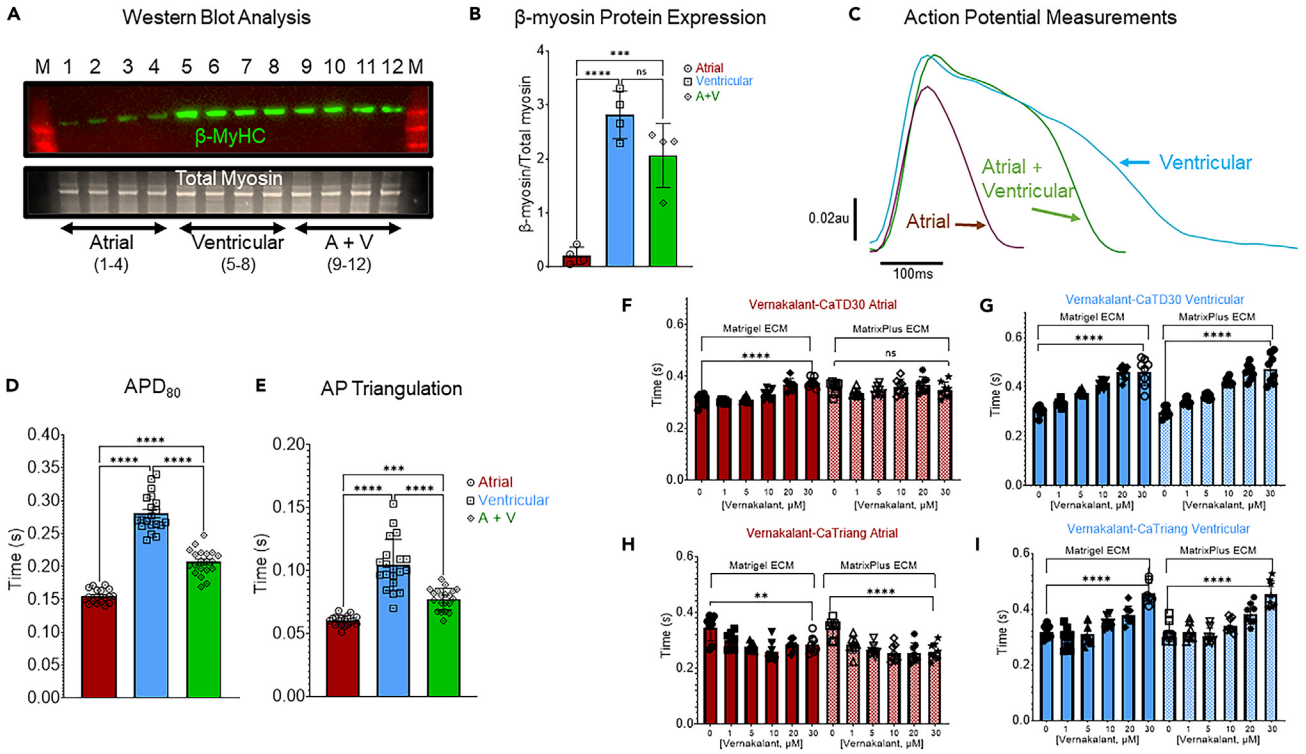

Figure 4. High-throughput electrophysiology analysis of chamber-specific hiPSC-CMs

(A) Western blot analysis of β-myosin heavy chain (β-MyHC) isoform expression in purified atrial-iPSC-CMs and purified ventricular-iPSC-CMs.

(B) Quantification of β-MyHC relative to total myosin indicates that ventricular hiPSC-CMs express significantly greater β-MyHC (2.81 ± 0.44au, n = 4 monolayer technical replicates) than atrial hiPSC-CMs (0.21 ± 0.16au, n = 4 monolayers). (One-way ANOVA, ****p < 0.0001; ***p = 0.0005).

(C and D) Optical mapping in 96-well plates, using voltage-sensitive dye (VSD, FluoVolt) confirms that atrial hiPSC-CM monolayers have shorter action potential duration (0.154 ± 0.01s, n = 18 monolayer technical replicates) than ventricular hiPSC-CMs (0.281 ± 0.03s, n = 20 monolayers) and monolayers made of 50% atrial and 50% ventricular hiPSC-CMs had average APD80 in between the two extremes (0.207 ± 0.02s, n = 20 monolayers). (One-way ANOVA, ****p < 0.0001).

(E) AP triangulation is greater in the ventricular monolayers (0.104 ± 0.02, n = 20 monolayers) than in atrial monolayers (0.060 ± 0.004, n = 18 monolayers) and heterogeneous monolayers of 50% atrial and 50% ventricular (A + V, 0.077 ± 0.008, n = 20 monolayers). (One-way ANOVA, ****p < 0.0001; ***p = 0.0006). For ANOVA post hoc analysis, Tukey's multiple comparisons test was used.

(F) Vernakalant dose response for effect on atrial CM CaTD30 plated on Matrigel (solid bars) or MatrixPlus (hashed bars).****p < 0.0001, unpaired t test 0 vernakalant vs. 30μM.

(G) Vernakalant dose response for the effect on ventricular CM CaTD30 plated on Matrigel (solid bars) or MatrixPlus (hashed bars). ****p < 0.0001, unpaired t test 0 vernakalant vs. 30μM.

(H) Dose response of vernakalant effect on Ca Triangulation (Ca Triang) in atrial CMs plated on Matrigel (solid bars) or MatrixPlus (hashed bars). ****p < 0.0001, **p = 0.008, unpaired t test 0 vernakalant vs. 30μM.

(I) Dose response of vernakalant effect on Ca Triangulation (Ca Triang) in ventricular CMs plated on Matrigel (solid bars) or MatrixPlus (hashed bars). ****p < 0.0001, unpaired t test, 0 vernakalant vs. 30μM. Data are expressed as mean ± standard deviation.

chamber-specific cardiac-directed differentiation.[39] Video S2 shows the difference of beat rate between atrial- and ventricular-specific CM monolayers, consistent with previous reports.[17] On day 20 of the differentiation protocol, purified hiPSC-CMs of either chamber type were obtained using magnetic assisted cell separation (MACS) and replated as confluent monolayers in a 96-well plate as recently described.[8] A molecular genetic hallmark of human cardiac chamber specificity is the myosin heavy chain isoform expression. The normal adult human atria express almost exclusively α-myosin heavy chain (α-MyHC) while the normal adult human ventricles express predominantly β-myosin heavy chain (β-MyHC).[40] Using a well-characterized β-MyHC-specific monoclonal antibody,[41,42] we probed for this ventricular-specific marker in hiPSC-CMs (Figures 4A and 4B) and found expression exclusively in the ventricular hiPSC-CMs. Total myosin was not different between atrial and ventricular hiPSC-CM monolayers, so by inference the atrial hiPSC-CMs expressed predominantly α-MyHC. In control experiments monolayers were generated consisting of a 50/50 mixture of each chamber-specific cell type (A + V). The A + V monolayers also expressed an intermediate amount of β-MyHC greater than the atrial CMs and less than the ventricular CMs.

Longitudinal directed contractions of rod-shaped atrial hiPSC-CMs were observed via video microscopy (Videos S3 and S4).

Next, we utilized the cardiac optical mapping plate reader to robustly characterize the AP profile of the chamber-specific hiPSC-CM monolayers. Consistent with reports using chamber-specific hiPSC-CMs and a wealth of knowledge of chamber-specific electrophysiology, atrial hiPSC-CM APD was significantly shorter than ventricular hiPSC-CMs APD (Figures 4C and 4D). Control monolayers consisting of a 50/50 mixture of A + V had average APD values in between APD values of atrial- and ventricular-specific hiPSC-CM monolayers. Similarly, AP triangulation was much less in atrial hiPSC-CMs, and the trends follow those for APD differences (Figure 4E). To further confirm chamber-specific drug response, we tested the effect of the atrial fibrillation-specific anti-arrhythmic medication, vernakalant (Figures 4F–4I and S10).[43,44] The high-throughput optical mapping enabled robust dose-response analysis for vernakalant with concentrations ranging from 1 to 30μM. Atrial hiPSC-CM monolayers CaTD30 was significantly increased at high dose of vernakalant while CaTD80 was not significantly altered. In ventricular hiPSC-CM monolayers, however, both CaTD30 and CaTD80 were both significantly prolonged to a greater degree than atrial monolayers. Notably, vernakalant reduced CaT triangulation of atrial cardiomyocyte monolayers but increased triangulation of ventricular cardiomyocyte monolayers (Figures 4H and 4I). Vernakalant slowed impulse conduction velocity in both atrial- and ventricular-specific monolayers (Figures S10C and S10D).

Cardiac EP plate reader: Validation and characterization of GECI-adenoviral delivery of GCaMP6 fast, medium, and slow variants with repeated measures

hiPSC-CM assays present the opportunity to determine the chronic effects of drugs on cardiac electrophysiological function. GECIs are an attractive option for repeated measures of electrophysiology and as a surrogate marker for contractile measurements in hiPSC-CM screening assays rather than using traditional VSDs and calcium-sensitive probes.[45,46] Here we used recombinant adenovirus to express GCaMP6 acutely in hiPSC-CM monolayers (Cellular Dynamics International, FUJIFILM). We tested the effect of three different GCaMP6 sensors, using three different adenoviruses: AdGCaMP6f (fast), AdGCaMP6m (medium), and AdGCaMP6s (slow) on hiPSC-CM function. The designations fast, medium, and slow refer to sensor calcium binding kinetics.[45] Our goal was to determine which GCaMP6 variant is optimal for use in hiPSC-CM assays.

Spontaneous CaTs were first observed one day after viral transduction and could be quantified using an inverted microscope (20fps, Cytation 5, BioTek, Figures 5A–5F and S11 and Video S5). Using the microscopic recordings, we found that GCaMP6 CaT amplitude increased between days 1–3 and was stable between days 3–8 following viral transduction (Figure S11A). Baseline fluorescence signals also increased over time following gene transfer and were significantly greater in hiPSC-CM monolayers expressing GCaMP6s (slow) compared to those transduced with GCaMP6 fast and medium variants (Figures S11C and S12A and Video S5). Importantly, on day 8 the total GCaMP6 protein expression was equal regardless of the virus used to express each variant: fast, medium, or slow (Figures S11D and S11E). Western Blot analysis indicated no difference of expression for the intracellular calcium pump, SERCA2a, in any group tested. Quantification of viral transduction efficiency for delivery of each GCaMP6 isoform indicated equal efficiency for each virus (Figure S12B).

Next, we utilized the cardiac EP plate reader to enable higher temporal resolution of the GECI CaTs. GCaMP6f, m, or s signal could be imaged using the cardiac EP plate reader starting on day three after gene transfer with repeated daily measures until day seven. This represents five days of repeated optical recordings without reloading the cells with dye and associated plate washes. After virus transduction, plates were transferred from the tissue culture incubator directly to the cardiac EP plate reader for CaT recordings (37°C, 100fps, 10s duration). CaTs were stable between days 3 and 7 when using the AdGCaMP6f virus, but hiPSC-CM monolayer function was more variable when using the AdGCaMP6s virus. These data are presented in Figures 5G–5W. On day 3 CaTD80 was significantly shorter in hiPSC-CM monolayers expressing the GCaMP6 fast isoform (0.517 $\pm$ 0.06s, n = 24) than in monolayers expressing the slow isoform (0.740 $\pm$ 0.05s, n = 24) and monolayers expressing the medium kinetic isoform (0.595 $\pm$ 0.05s, n = 24). These differences in CaTD80 persisted between the GCaMP6 variant expressing hiPSC-CMs, but the magnitude of the difference decreased by day seven (day 7 CaTD80: AdGCaMP6f = 0.451 $\pm$ 0.06s; AdGCaMP6m = 0.496 $\pm$ 0.06s; AdGCaMP6s = 0.507 $\pm$ 0.07s, n = 24 monolayers per group). AdGCaMP6s-expressing monolayers' spontaneous beat rate was the greatest of the

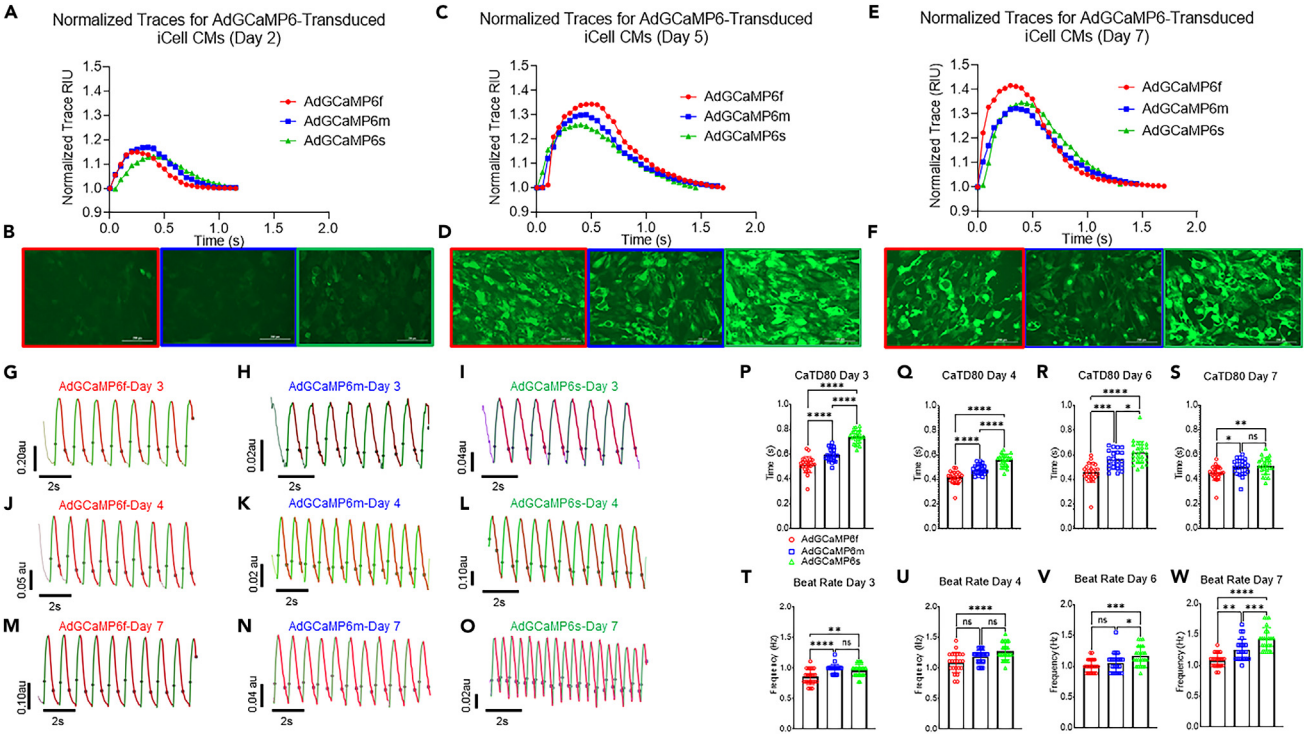

Figure 5. Characterization of GCaMP6 variants effects on hiPSC-CM electrophysiological function with repeated measures

(A) Representative calcium transient traces recorded on day 2 following AdGCaMP6f, m, or s viral transduction in commercially available hiPSC-CMs (iCell,[2] Cellular Dynamics International) using a widefield fluorescence microscope.

(B) Day 2 microscopic images of monolayers' baseline green fluorescence for each GCaMP6 variant: red = fast, blue = medium and green = slow.

(C) Calcium transients recorded on day 5 following adenoviral transduction of each GCaMP6 variant.

(D) Day 5 microscopic images of monolayers' baseline green fluorescence for each GCaMP6 variant.

(E) Calcium transients recorded on day 7 following adenoviral transduction of each GCaMP6 variant.

(F) Day 7 microscopic images of monolayers' baseline green fluorescence for each GCaMP6 variant.

(G–I) Representative CARTOX optical recordings of hiPSC-CM calcium transients on day 3 after adenoviral transduction of each GCaMP6 variant.

(J–L) Day 4 representative recordings of calcium transients and M-O show Day 7 recordings of each GCaMP6 variant.

(P–S) Quantification of calcium transient duration 80 (CaTD80) for each variant at days 3–7. (One-way ANOVA, ****$p < 0.0001$, ***$p = 0.0002$, **$p < 0.008$, *$p < 0.05$, n = 24 monolayer technical replicates per group).

(T–W) Quantification of hiPSC-CM spontaneous beat rate days 3–7 following adenoviral transduction of each GCaMP6 variant. (One-way ANOVA, ****$p < 0.0001$, ***$p = 0.0002$, **$p < 0.008$, *$p < 0.05$, n = 24 monolayers per group). For ANOVA post hoc analysis, Tukey's multiple comparisons test was used. Data are expressed as mean ± standard deviation.

three variants on day 3 (AdGCaMP6f = 0.86 ± 0.12s; AdGCaMP6m = 0.99 ± 0.08s; AdGCaMP6s = 0.96 ± 0.09s, n = 24 monolayers per group). The difference of spontaneous beat rate between the groups was even greater at day seven (AdGCaMP6f = 1.08 ± 0.11Hz; AdGCaMP6m = 1.25 ± 0.17Hz; AdGCaMP6s = 1.44 ± 0.18s, n = 24 monolayers per group).

We determined the effect of GCaMP6 variant expression on hiPSC-CM monolayer β-adrenergic stimulation responsiveness using acute ISO application (0.10μM; Figures 6A–6F). This comparison was made on day six following adenoviral gene transfer using the cardiac EP plate reader. Analysis is paired with quantification of the same well function before and after acute ISO treatment. AdGCaMP6f-treated monolayers' spontaneous beat rate (Hz) and CaT amplitude (ΔF/F) both increased with ISO treatment. AdGCaMP6m- and s-expressing monolayers' spontaneous beat rate increased, but CaT amplitudes did not increase with ISO treatment. CaTD80 decreased with ISO in all monolayers regardless of GCaMP6 variant expression. Finally, we tested responsiveness to the hERG channel blocker, E−4031 (0.2μM; Figures 6G–6L). E−4031 slowed beat rate and increased CaTD80 regardless of GCaMP6 variant expression. AdGCaMP6f-expressing monolayers' CaT amplitude was reduced with E−4031 treatment but was unaffected in monolayers expressing the medium and slow GCaMP6 variants.

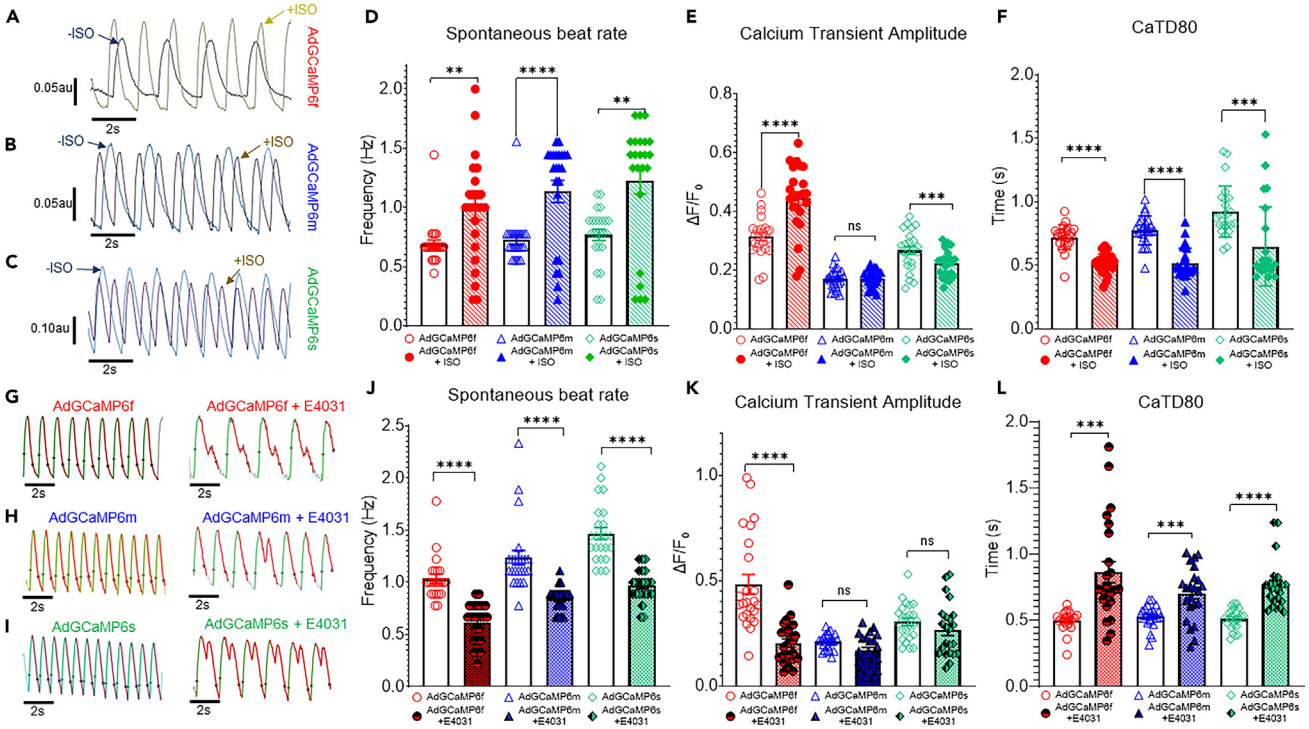

Figure 6. AdGCaMP6 variant effect on hiPSC-CM responsiveness to two classical cardioactive compounds on day 6 following viral transduction

(A–C) representative well traces of calcium transient responses to isoproterenol (+ISO, 0.10μM) stimulation. –ISO indicates traces before treatment +ISO indicates the same well traces immediately following ISO treatment for each GCaMP6 variant (A, red = AdGCaMP6f; B, blue = AdGCaMP6; C, green = AdGCaMP6s.

(D) Paired analysis of the spontaneous beat rate for each virus treatment before and after ISO.

(E) Paired analysis for the effect of ISO on the calcium transient amplitude (ΔF/F0) in each virus-treated group.

(F) Paired analysis for the effect of ISO on the CaTD80 in each virus-treated group. (For D-F; Paired t tests, ****$p < 0.0001$; ***$p \leq 0.002$, n = 23–24 monolayer technical replicates per group).

(G–I) Representative well traces of calcium transient responses to E−4031 (0.2μM) for each GCaMP6 variant.

(J) Paired analysis of the effect of E−4031 on hiPSC-CM spontaneous beat rate.

(K) Paired analysis of the effect of E−4031 on the calcium transient amplitude for each virus-treated group.

(L) Paired analysis for the effect of E−4031 on the CaTD80 for each group. (For J-L, Paired t tests, ****$p < 0.0001$, ***$p \leq 0.002$, n = 23–24 monolayers per group). Data are expressed as mean ± standard deviation.

Finally, we utilized the GCaMP6f calcium indicator to determine the effect of daily ISO pulses (0.2μM) on hiPSC-CM monolayer electrophysiological function and SERCA2a protein expression (Figure 7). In one set of monolayers, ISO was added daily with subsequent washout over a period of four days (Figure 7A, n = 16). In the control group, vehicle control media was added (DMSO) in place of ISO (Figure 7A, n = 8). On each day spontaneous CaTs were recorded before and after ISO treatment to confirm effectiveness to increase the spontaneous beat rate (Figure 7A). Successful washout of the ISO was evident on each day, providing assurance of the pulsing of β-adrenergic receptor activation. On day five of these experiments baseline recordings were taken using the cardiac EP plate reader to determine effects on the function of hiPSC-CM monolayers. Daily pulsing of ISO impacted the baseline function: spontaneous beat rate was increased, duration was decreased, conduction velocity increased, and triangulation decreased compared to time-matched control monolayers treated with vehicle media (Figures 7C–7H). Western blot analysis showed that SERCA2a protein expression was elevated in monolayers pulsed daily with ISO (Figures 7I and 7J). Washout of the daily ISO pulse was also confirmed by western blot, probing for phospho-cTnI (Figure 7I). On day 5, the basal level of cTnI phosphorylation was the same between groups. Upon acute ISO treatment in each group, the extent of cTnI phosphorylation was not different. Positive chronotropic effect of ISO was more apparent in ISO-pulsed monolayers than control (Figure 7K). Conduction velocity reached greater values following ISO treatment in ISO-pulsed monolayers compared to control (Figure 7L).

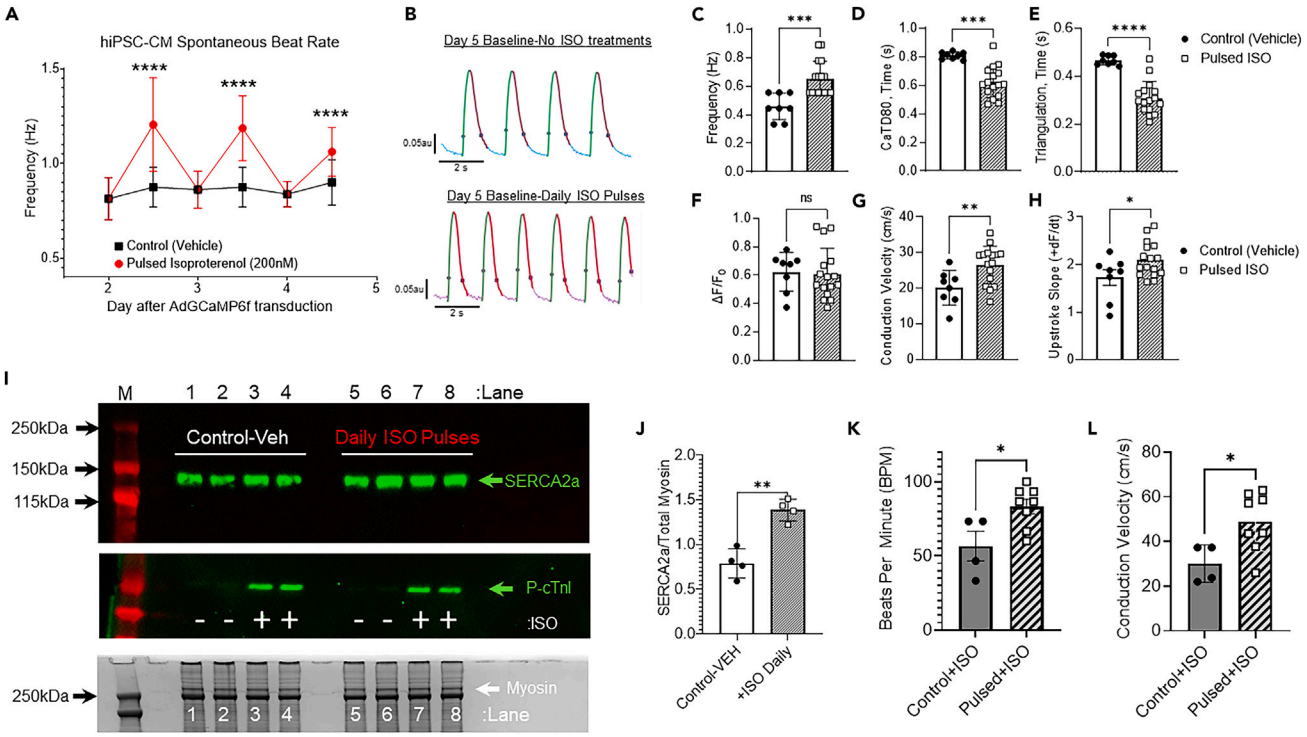

Figure 7. GCaMP6f repeated measures to determine effect of daily isoproterenol pulses on hiPSC-CM function

(A) Daily measurement of GCaMP6f spontaneous calcium flux in hiPSC-CM monolayers confirmed pulsing of isoproterenol (0.2μM). At each time point, isoproterenol-treated monolayers' spontaneous beat rate increased significantly (red symbols, n = 21; ****p < 0.0001, unpaired t test compared to control, vehicle treated, n = 8, black symbols).

(B) On day 5 of this protocol baseline recordings of spontaneous activity was recorded using the cardiac EP plate reader; these are representative traces from each group. Upstroke of the calcium transient is automatically determined and colored green while the calcium transient decay from peak is labeled red.

(C) Isoproterenol pulsing increased spontaneous beat rate (Pulsed ISO = 0.65 ± 0.12Hz, n = 8 vs. Control (Vehicle) = 0.46 ± 0.09Hz, n = 16 monolayer technical replicates; ***p = 0.0006, unpaired t test).

(D) CaTD80 was shorter in ISO-pulsed monolayers (0.623 ± 0.11s, n = 16) relative to control (0.809 ± 0.02s, n = 8); ***p = 0.0006, unpaired t test.

(E) Calcium transient triangulation was significantly less in ISO-pulsed monolayers (0.309 ± 0.07s, n = 16) compared to control (0.467 ± 0.02s, n = 8) ****p < 0.0001, unpaired t test.

(F) Calcium transient amplitude was not different at baseline between the two groups.

(G) Conduction velocity was greater in monolayers pulsed daily with ISO (26.4 ± 5.3 cm/s, n = 16 vs. 20.1 ± 4.9 cm/s, n = 8; **p = 0.009, unpaired t test).

(H) Calcium transient upstroke slope (+dF/dt) was faster in ISO-pulsed monolayers.

(I) Western blot analysis probing for SERCA2a expression (top) and phospho-cTnI (middle). Total protein stain (bottom) used for normalization and equal protein loading control.

(J) SERCA2a protein expression on day 5 was greater in monolayers treated daily with ISO. **p = 0.001, unpaired t test, n = 4 per group.

(K) In response to acute ISO on day 5, pulsed monolayers beat rate increased to a greater value than control (83.3 ± 13.8 beat per minute (BPM), n = 8 vs. 56.67 ± 20.0BPM, n = 4).

(L) Conduction velocity increased to greater values following acute ISO treatment in monolayers with a history of ISO pulsing (48.9 ± 13.2 cm/s, n = 8 vs. 30.1 ± 8.4 cm/s, n = 4 technical replicates) *p = 0.02, unpaired t tests. Data are expressed as mean ± standard deviation.

DISCUSSION

A major criticism hindering the widespread use and acceptance of hiPSC-CMs for pre-clinical *in vitro* cardiotoxicity screening and biomedical research has been the immature, fetal-like structure of the cells.[4] Here we have expanded on a previous report[20] and solved this limitation using a human perinatal stem cell-derived ECM coating for standard high-throughput 96 well cell culture plates. Further, we have developed and fully validated an automated high-throughput cardiac EP plate reader capable of recording APs or CaTs from an entire 96-well plate in 5 min. Cardiac EP readings were validated using drug compounds with known effects and using multiple hiPSC-CM lines. Importantly, here we utilized mature hiPSC-CMs to provide important new biological insight into the use of GECI for functional phenotype analysis and medication screening with repeated measures over a seven-day period. Repeated measures using GECI enabled daily interrogation and confirmation of hiPSC-CM monolayer functional response to ISO pulses

over a four-day period. We discovered that daily ISO pulses altered the baseline function and increased SERCA2a protein expression in hiPSC-CM 2D monolayers. The advances reported here using standard 2D cell culture approaches provide a highly feasible solution to the problem of hiPSC-CM maturation and high-throughput electrophysiological screening using cardiac optical mapping approaches.

ECM cues have profound impact on cellular behavior and maturation.[47,48] ECM modulations have been reported to significantly mature the structural and functional phenotypes of hiPSC-CMs *in vitro*.[18,20,22] Here we report the first high-throughput automated production and use of human ECM-coated cell culture plates specifically designed for hiPSC-CM screening assays. Human ECM-coated cell culture plates (CELLvo MatrixPlus, StemBioSys, Inc.) promoted significant maturation of hiPSC-CM toward rod-shaped cells reminiscent of cardiomyocytes isolated from adult mammalian hearts (Figures 1 and S1–S4). hiPSC-CM sarcomere length was longer and more organized in cells maintained on MatrixPlus-human ECM (Figures 1C and 1D). Importantly, MatrixPlus maturation effects were reproducible using multiple hiPSC lines (Figure 1F). Besides these structural markers of maturation, MatrixPlus ECM also promoted functional maturation of hiPSC-CM monolayers in these small format wells (~9mm diameter, 96-well plates). MatrixPlus ECM increased mitochondrial membrane polarization in hiPSC-CMs compared to CMs maintained on Matrigel ECM (Figures 1A, 1B, and S1). The JC-1 data indicate more polarized mitochondrial membrane potential in hiPSC-CMs plated and maintained on MatrixPlus-human ECM. Conduction velocity of hiPSC-CM monolayers plated on MatrixPlus was rapid (Figure 2D, ~45 cm s^{-1}), near values reported for whole hearts *in vivo*. This is a major advance over other high-content *in vitro* maturation approaches where hiPSC-CM impulse conduction velocity has fallen short of expectations (up to ~25 cm s^{-1}).[21] Reports on hiPSC-CM response to positive inotropic reagents have been highly variable and are not directly measured in many multi-electrode- and impedance-based assays.[49] Importantly, the mature hiPSC-CM monolayer response to the positive chronotropic and inotropic agent, ISO, here is similar to the response of the whole heart and mature cardiomyocytes (Figures 3A–3E and 6A).[41] Indeed, hiPSC-CM maturation is robust, and responses to medications are like adult heart responses when cells are matured using MatrixPlus-human ECM.

High-throughput electrophysiological screening assays using mature hiPSC-CMs are required to position the *in vitro* assays in the drug development process. Different functional readout approaches have been utilized for hiPSC-CM proarrhythmic and cardiotoxicity screening including MEAs and VSD assays.[5,32] MEA assays utilize expensive specialized cell culture plates that have golden electrodes engineered into each well of a multi-well plate. A strength of MEA approaches is repeated measurements without the need for labeling cells. However, a major weakness of the MEA approach is low spatial resolution of recording. For example, using 96-well plate MEA assays there are only 8 electrodes per well and only the electrodes with good contact to cells are usable. This leads to selection of a single useful electrode in some cases to represent an entire well response to a drug. Impulse conduction is also difficult to quantify using MEA where the limited numbers of recording electrodes are spaced far apart relative to the size of a single cardiomyocyte. On the other hand, cardiac optical mapping assays offer much higher spatial resolution data, limited only by the camera sensor resolution. Here we used a camera pixel resolution yielding 76,800 pixels per well of each 96-well plate combined with high frame rate acquisition (100-500fps). Optical-based recording approaches yield orders of magnitude greater data resolution per well compared to MEA assays. Here we utilized the cardiac EP plate reader for multiple biological applications including confirmation of cardiac chamber specificity, optimization of using GECI for repeated measures, and to determine the effect of daily ISO pulses on hiPSC-CM function and protein expression.

Cardiac chamber-specific differentiation was tested at the molecular level by probing for the ventricular-specific β-MyHC isoform protein expression (Figures 4A and 4B) or the atrial-specific myosin light chain 2a expression (Figure S9). This is the first report to our knowledge of using myosin heavy chain isoform protein expression to discriminate between atrial- and ventricular-specific hiPSC-CMs. We utilized the cardiac EP plate reader to robustly confirm the chamber specificity of the differentiation protocol (Figures 4C–4I). Consistent with other reports atrial APD was significantly shorter than ventricular hiPSC-CM APD.[50] Control monolayers consisting of 50/50 atrial and ventricular CMs had APD values in between the pure atrial and pure ventricular numbers. Vernakalant, a medication with chamber-specific effects used to treat atrial fibrillation[51] was used to further verify chamber specificity (Figures 4F–4I and S10). In atrial-specific hiPSC-CM monolayers vernakalant prolonged CaTD30 (Figure 4F) significantly but not CaTD80 (Figure S10). On the other hand, vernakalant increased CaTD30 and CaTD80 in ventricular-specific hiPSC-CMs. This translated

to an effect of vernakalant to reduce CaT triangulation in atrial CM monolayers but to increase triangulation of ventricular CM monolayers (Figures 4H and 4I). Triangulation is an index of proarrhythmic potential; reagents that reduce triangulation are considered anti-arrhythmic,[52] so our data indicate that vernakalant may be anti-arrhythmic in atrial CMs but may be proarrhythmic in ventricular CMs. This underscores the critical need for chamber specificity of hiPSC-CM assays used for safety pharmacology and cardiotoxicity screening.

A limitation of using optical-based recording for hiPSC-CM repeated measures has been the need for repeated loading of VSDs or calcium-sensitive probes in hiPSC-CMs required due to loss of signal over time. The repeated loading of chemical probes across cell membranes can cause cytotoxicity and thus preclude meaningful repeated measures of functionality. To enable repeated optical recordings of hiPSC-CM electrophysiological function, here we optimized the use of GECI. A commonly used GECI is GCaMP, a synthetic fusion of GFP (green fluorescent protein), calmodulin (CaM), and M13, a peptide sequence from myosin light chain kinase.[46] Different GCaMP6 variants have been developed: GCaMP6-fast(f), GCaMP6medium(m), and GCaMP6slow(s).[45] Kinetic designations indicate the rate of calcium binding and unbinding from the probe. GCaMP6s (slow) has been used for hiPSC-CM cell functional measurements.[53,54] Jiang et al.[53] generated a GCaMP6s knockin hPSC line, differentiated the stem cells to cardiomyocytes, and could detect the CaTs of hPSC-derived CMs. Another variant, GCaMP5G, has also been used to monitor hiPSC-CM calcium flux and drug responsiveness.[55] Here we provide the first optimization of GCaMP6 variant selection (fast, medium, and slow) for repeated measures of hiPSC-CM electrophysiological and contractile functions. We utilized recombinant adenoviruses for acute GCaMP6 gene transfer in hiPSC-CM monolayers (iCell Cardiomyocytes[2]) under the control of cytomegalovirus (CMV) promoter. hiPSC-CM calcium flux kinetics were determined by the kinetics of the GCaMP6 sensor. Specifically, in GCaMP6s-treated monolayers CaTD was significantly greater throughout the period of recording than for the fast and medium GCaMP6 variants (e.g., day 3, GCaMP6s CaTD80 = 0.740 $\pm$ 0.05s; GCaMP6m CaTD80 = 0.595 $\pm$ 0.05s; GCaMP6f CaTD80 = 0.516 $\pm$ 0.06s n = 24 monolayers per group). This cannot be attributed to differences of each sensor expression, Western blotting confirmed equal expression of each GCaMP6 variant in hiPSC-CMs and showed that calcium pump expression (SERCA2a) was the same in all groups (Figure S11). Prolongation of the CaTD is a well-known cellular dysfunction associated with cardiovascular diseases like heart failure.[56,57] The elevated baseline fluorescence in the case of the GCaMP6s variant also indicates buildup of cytosolic calcium levels relative to the hiPSC-CM monolayers expressing the fast and medium variants (Figure S12A). Elevated baseline cytosolic calcium levels in the GCaMP6s-transduced hiPSC-CM monolayers are predicted to depolarize the membrane potential closer to the threshold for AP firing, resulting in the observed elevation of spontaneous beating rate in the GCaMP6s group compared to the GCaMP6f and m groups (Figure 5W). Figure 6 provides important new insight into the impact of GCaMP6 kinetic variants on cardiac drug responsiveness. ISO increased the spontaneous beat rate in hiPSC-CM monolayers independent of GCaMP6 variant expression (Figure 6D) as expected. ISO also shortened the duration of the CaT independent of the GCaMP6 variant (Figure 6F). However, when measuring the effect of ISO on contractility, the GCaMP6m and GCaMP6s variants showed abnormal response to this positive inotropic agent. Only monolayers expressing the GCaMP6f variant displayed increase of CaT amplitude upon β-adrenergic stimulation with ISO, a classical response of the heart and single adult cardiomyocytes (Figure 6E). Thus, hiPSC-CM cardiotoxicity screening assays utilizing GCaMP6f GECI provide a robust assay with stable function over at least seven days and expected physiological responses to G-protein-coupled receptor activation. GCaMP6m and s variants, on the other hand, cause pathophysiological responses in hiPSC-CMs and may be considered for creating disease models of calcium overload. Using the high-throughput cardiac EP plate reader, we very rapidly and robustly optimized the use and selection of GECI to provide an optically based hiPSC-CM assay with the option for repeated measures.

Finally, the use of GCaMP6f enabled us to determine the effect of daily ISO pulses on hiPSC-CM monolayer electrophysiological function (Figure 7). Daily pulses of ISO (200nM) were confirmed (via microscopy) with daily CaT recordings to observe the chronotropic effect of the drug. At the end of the ISO pulsing regimen baseline spontaneous beating function was recorded using the cardiac EP plate reader. Pulsing ISO increased the functional maturation of hiPSC-CMs further, evidenced by reduced CaTD and increased impulse conduction velocity (Figures 7C–7H). Western blot analysis revealed that ISO pulsing increased the SERCA2a protein expression level (Figures 7I and 7J). Elevated SERCA2a expression is a mechanism that

underlies the hastening of CaTD in the ISO-pulsed group. Interestingly, ISO pulsing did not alter the baseline levels of phospho-cTnI and did not alter the extent of cTnI phosphorylation upon acute ISO application (Figure 7I). Detection of phospho-cTnI here also provides a molecular marker of hiPSC-CM maturation. cTnI protein expression is a recognized genetic molecular marker for hiPSC-CM maturation.[58] cTnI and thus phospho-cTnI are not detectable in fetal-like cardiomyocytes. This corroborates previous reports of robust cTnI expression induced by the MatrixPlus ECM, relative to hiPSC-CMs maintained on Matrigel.[20] Acute ISO application to the ISO-pulsed group revealed increased functional responsiveness, indicating an increased gain of the adrenergic receptor signaling pathway (Figures 7K and 7L). Thus, daily ISO pulsing represents a new approach for hiPSC-CM maturation of intracellular calcium handling mechanisms. Daily administration of a medication (ISO) to chemically stimulate a specific signaling pathway offers advantages over other chronic nonspecific perturbations like electrical pacing[30] and mechanical stretching.[59] Electrical pacing and mechanical stretching require complex engineering tools to implement; on the other hand application of a chemical like ISO is simple to implement and does not require sophisticated instrumentation to complete.

Limitations of the study

Despite the convincing degree of maturation reported here, there are limitations to the current study and approach to *in vitro* cardiotoxicity and electrophysiological screening. First, we have not quantified every aspect of cardiac maturation. Other aspects of maturation including binucleation, oxygen consumption rate, response to parasympathetic agonists like acetylcholine, t-tubule formation, and membrane potential quantification have not been measured here. Second, this system does not directly measure contraction but uses the CaT amplitude as a surrogate marker for contractility. This prevents direct measurement of cardiac excitation-contraction coupling. Direct measurement of contraction requires growing the cells on specialized surfaces equipped with contraction sensors or the generation of 3D engineered heart tissues.[29,30,60,61] 3D engineered heart tissues also develop t-tubules, though it should be pointed out that the use of 3D EHTs requires many more cells than 2D monolayers and often requires the inclusion of non-myocytes which can have impact on function. On the other hand, 2D monolayers utilize purified hiPSC-CMs, thus avoiding complications presented by co-culture. Third, the hiPSC-CM monolayers here have not been electrically paced; rather the system relies on the spontaneous beating of the hiPSC-CM monolayers. Finally, a greater number of patients hiPSC lines need to be tested using this approach for cardiomyocyte maturation to be certain that it applies broadly to human cardiomyocyte monolayers.

STAR★METHODS

Detailed methods are provided in the online version of this paper and include the following:

- KEY RESOURCES TABLE
- RESOURCE AVAILABILITY
  - Lead contact
  - Materials availability
  - Data and code availability
- EXPERIMENTAL MODEL AND STUDY PARTICIPANT DETAILS
  - Cell lines
- METHOD DETAILS
  - Human extracellular matrix (ECM) production
  - Cardiac EP plate reader prototype and analysis software
  - Experimental models: hiPSC-CM cell sources
  - Fluorescent staining and microscopy
  - Cardiac EP plate reader for action potential and calcium transient analysis
  - GCaMP6fast, medium or slow variant acute gene transfer
  - Western blot analysis
  - Drug/medication testing
- QUANTIFICATION AND STATISTICAL ANALYSIS

SUPPLEMENTAL INFORMATION

Supplemental information can be found online at https://doi.org/10.1016/j.isci.2023.107142.

ACKNOWLEDGMENTS

The research was supported by the National Institutes of Health grants R44ES027703, R01HL148068 (to T.J.H), UH3TR003271, R01HL146436, R01HL156947, and R01HL164936 (to D.-H.K.). Additional funding from NSF-CELL MET grant (NSF Engineering Research Center in Cellular Metamaterials) supported the project. T.J.H also received funding from the US-Israel Binational Science Foundation. The authors would like to also acknowledge Coby Carlson (FUJIFILM, CDI) for testing and feedback regarding use of the cardiac EP plate reader and Jiang Jiang and Noreen Herron for assistance with set up and shipping/transportation of the plate reader.

AUTHOR CONTRIBUTIONS

A.A. designed and constructed the Cardiac EP plate reader. J.C., A.M.R., and D.B.M. plated cardiomyocytes, differentiated iPSCs to cardiomyocytes, purified cardiomyocytes, and replated pure cardiomyocytes as confluent monolayers in 96-well plates for analysis. C.H., P.K., R.D., and T.J.H. imaged and analyzed live monolayers' calcium transients using the Cytation 5 imager. B.G., C.H., R.D., and P.K. performed western blot analysis and quantification. T.B. generated human ECM-coated cell culture plates and performed quality control on coated culture plates. T.J.H wrote the manuscript in collaboration with all the authors and performed cardiac EP analysis and confocal imaging of hiPSC-CMs. T.J.H and D.-H.K. conceived and supervised the project, designed experiments, and analyzed and interpreted the data.

DECLARATION OF INTERESTS

T.J.H. is a consultant to StemBioSys, Inc. and is a member of the Scientific Advisory Board. A.M.R., J.C., T.J.H., and T.B. have ownership stake in StemBioSys, Inc. T.B. is an employee of StemBioSys, Inc. A.A. is an employee of CAIRN Research. D.-H.K. is a scientific founder and equity holder of Curi Bio.

Received: September 8, 2022
Revised: June 1, 2023
Accepted: June 12, 2023
Published: June 15, 2023

REFERENCES

1. Zhang, J., Wilson, G.F., Soerens, A.G., Koonce, C.H., Yu, J., Palecek, S.P., Thomson, J.A., and Kamp, T.J. (2009). Functional cardiomyocytes derived from human induced pluripotent stem cells. Circ. Res. *104*, e30–e41.

2. Thomson, J.A., Itskovitz-Eldor, J., Shapiro, S.S., Waknitz, M.A., Swiergiel, J.J., Marshall, V.S., and Jones, J.M. (1998). Embryonic stem cell lines derived from human blastocysts. Science *282*, 1145–1147.

3. Takahashi, K., Tanabe, K., Ohnuki, M., Narita, M., Ichisaka, T., Tomoda, K., and Yamanaka, S. (2007). Induction of pluripotent stem cells from adult human fibroblasts by defined factors. Cell *131*, 861–872.

4. Ahmed, R.E., Anzai, T., Chanthra, N., and Uosaki, H. (2020). A Brief Review of Current Maturation Methods for Human Induced Pluripotent Stem Cells-Derived Cardiomyocytes. Front. Cell Dev. Biol. *8*, 178.

5. Blinova, K., Dang, Q., Millard, D., Smith, G., Pierson, J., Guo, L., Brock, M., Lu, H.R., Kraushaar, U., Zeng, H., et al. (2018). International Multisite Study of Human-Induced Pluripotent Stem Cell-Derived Cardiomyocytes for Drug Proarrhythmic Potential Assessment. Cell Rep. *24*, 3582–3592.

6. da Rocha, A.M., Creech, J., Thonn, E., Mironov, S., and Herron, T.J. (2020). Detection of Drug-Induced Torsades de Pointes Arrhythmia Mechanisms Using hiPSC-CM Syncytial Monolayers in a High-Throughput Screening Voltage Sensitive Dye Assay. Toxicol. Sci. *173*, 402–415.

7. Yang, X., Ribeiro, A.J.S., Pang, L., and Strauss, D.G. (2022). Use of Human iPSC-CMs in Nonclinical Regulatory Studies for Cardiac Safety Assessment. Toxicol. Sci. *190*, 117–126.

8. Davis, J., Chouman, A., Creech, J., Monteiro da Rocha, A., Ponce-Balbuena, D., Jimenez Vazquez, E.N., Nichols, R., Lozhkin, A., Madamanchi, N.R., Campbell, K.F., and Herron, T.J. (2021). In vitro model of ischemic heart failure using human induced pluripotent stem cell-derived cardiomyocytes. JCI Insight *6*, e134368.

9. Lan, F., Lee, A.S., Liang, P., Sanchez-Freire, V., Nguyen, P.K., Wang, L., Han, L., Yen, M., Wang, Y., Sun, N., et al. (2013). Abnormal calcium handling properties underlie familial hypertrophic cardiomyopathy pathology in patient-specific induced pluripotent stem cells. Cell Stem Cell *12*, 101–113.

10. Feng, L., Zhang, J., Lee, C., Kim, G., Liu, F., Petersen, A.J., Lim, E., Anderson, C.L., Orland, K.M., Robertson, G.A., et al. (2021). Long QT Syndrome KCNH2 Variant Induces hERG1a/1b Subunit Imbalance in Patient-Specific Induced Pluripotent Stem Cell-Derived Cardiomyocytes. Circ. Arrhythm. Electrophysiol. *14*, e009343.

11. Eisen, B., Ben Jehuda, R., Cuttitta, A.J., Mekies, L.N., Shemer, Y., Baskin, P., Reiter, I., Willi, L., Freimark, D., Gherghiceanu, M., et al. (2019). Electrophysiological abnormalities in induced pluripotent stem cell-derived cardiomyocytes generated from Duchenne muscular dystrophy patients. J. Cell Mol. Med. *23*, 2125–2135.

12. Kawamura, M., Miyagawa, S., Miki, K., Saito, A., Fukushima, S., Higuchi, T., Kawamura, T., Kuratani, T., Daimon, T., Shimizu, T., Okano, T., and Sawa, Y. (2012). Feasibility, safety, and therapeutic efficacy of human induced pluripotent stem cell-derived cardiomyocyte sheets in a porcine ischemic cardiomyopathy model. Circulation *126*, S29–S37.

13. Liew, L.C., Ho, B.X., and Soh, B.-S. (2020). Mending a broken heart: current strategies and limitations of cell-based therapy. Stem Cell Res. Ther. *11*, 138.

14. Blinova, K., Schocken, D., Patel, D., Daluwatte, C., Vicente, J., Wu, J.C., and Strauss, D.G. (2019). Clinical Trial in a Dish: Personalized Stem Cell–Derived Cardiomyocyte Assay Compared With

Clinical Trial Results for Two QT-Prolonging Drugs. Clin. Transl. Sci. *12*, 687–697.

15. Strauss, D.G., and Blinova, K. (2017). Clinical Trials in a Dish. Trends Pharmacol. Sci. *38*, 4–7.

16. Ma, J., Guo, L., Fiene, S.J., Anson, B.D., Thomson, J.A., Kamp, T.J., Kolaja, K.L., Swanson, B.J., and January, C.T. (2011). High purity human-induced pluripotent stem cell-derived cardiomyocytes: electrophysiological properties of action potentials and ionic currents. Am. J. Physiol. Heart Circ. Physiol. *301*, H2006–H2017.

17. Cyganek, L., Tiburcy, M., Sekeres, K., Gerstenberg, K., Bohnenberger, H., Lenz, C., Henze, S., Stauske, M., Salinas, G., Zimmermann, W.-H., et al. (2018). Deep phenotyping of human induced pluripotent stem cell-derived atrial and ventricular cardiomyocytes. JCI Insight *3*, e99941.

18. Herron, T.J., Rocha, A.M.D., Campbell, K.F., Ponce-Balbuena, D., Willis, B.C., Guerrero-Serna, G., Liu, Q., Klos, M., Musa, H., Zarzoso, M., et al. (2016). Extracellular Matrix-Mediated Maturation of Human Pluripotent Stem Cell-Derived Cardiac Monolayer Structure and Electrophysiological Function. Circ. Arrhythm. Electrophysiol. *9*, e003638.

19. Blinova, K., Stohlman, J., Vicente, J., Chan, D., Johannesen, L., Hortigon-Vinagre, M.P., Zamora, V., Smith, G., Crumb, W.J., Pang, L., et al. (2017). Comprehensive Translational Assessment of Human-Induced Pluripotent Stem Cell Derived Cardiomyocytes for Evaluating Drug-Induced Arrhythmias. Toxicol. Sci. *155*, 234–247.

20. Block, T., Creech, J., da Rocha, A.M., Marinkovic, M., Ponce-Balbuena, D., Jiménez-Vázquez, E.N., Griffey, S., and Herron, T.J. (2020). Human perinatal stem cell derived extracellular matrix enables rapid maturation of hiPSC-CM structural and functional phenotypes. Sci. Rep. *10*, 19071.

21. Smith, A.S.T., Choi, E., Gray, K., Macadangdang, J., Ahn, E.H., Clark, E.C., Laflamme, M.A., Wu, J.C., Murry, C.E., Tung, L., and Kim, D.H. (2020). NanoMEA: A Tool for High-Throughput, Electrophysiological Phenotyping of Patterned Excitable Cells. Nano Lett. *20*, 1561–1570.

22. Feaster, T.K., Cadar, A.G., Wang, L., Williams, C.H., Chun, Y.W., Hempel, J.E., Bloodworth, N., Merryman, W.D., Lim, C.C., Wu, J.C., et al. (2015). Matrigel Mattress: A Method for the Generation of Single Contracting Human-Induced Pluripotent Stem Cell-Derived Cardiomyocytes. Circ. Res. *117*, 995–1000.

23. Dhahri, W., Sadikov Valdman, T., Wilkinson, D., Pereira, E., Ceylan, E., Andharia, N., Qiang, B., Masoudpour, H., Wulkan, F., Quesnel, E., et al. (2022). In Vitro Matured Human Pluripotent Stem Cell–Derived Cardiomyocytes Form Grafts With Enhanced Structure and Function in Injured Hearts. Circulation *145*, 1412–1426.

24. Kamakura, T., Makiyama, T., Sasaki, K., Yoshida, Y., Wuriyanghai, Y., Chen, J., Hattori, T., Ohno, S., Kita, T., Horie, M., Yamanaka, S., and Kimura, T. (2013). Ultrastructural Maturation of Human-Induced Pluripotent Stem Cell-Derived Cardiomyocytes in a Long-Term Culture. Circ. J. *77*, 1307–1314.

25. Lundy, S.D., Zhu, W.-Z., Regnier, M., and Laflamme, M.A. (2013). Structural and functional maturation of cardiomyocytes derived from human pluripotent stem cells. Stem Cell. Dev. *22*, 1991–2002.

26. Lewandowski, J., Rozwadowska, N., Kolanowski, T.J., Malcher, A., Zimna, A., Rugowska, A., Fiedorowicz, K., Łabędź, W., Kubaszewski, Ł., Chojnacka, K., et al. (2018). The impact of in vitro cell culture duration on the maturation of human cardiomyocytes derived from induced pluripotent stem cells of myogenic origin. Cell Transplant. *27*, 1047–1067.

27. da Rocha, A.M., Campbell, K., Mironov, S., Jiang, J., Mundada, L., Guerrero-Serna, G., Jalife, J., and Herron, T.J. (2017). hiPSC-CM Monolayer Maturation State Determines Drug Responsiveness in High Throughput Pro-Arrhythmia Screen. Sci. Rep. *7*, 13834.

28. Almeida, H.V., Tenreiro, M.F., Louro, A.F., Abecasis, B., Santinha, D., Calmeiro, T., Fortunato, E., Ferreira, L., Alves, P.M., and Serra, M. (2021). Human Extracellular-Matrix Functionalization of 3D hiPSC-Based Cardiac Tissues Improves Cardiomyocyte Maturation. ACS Appl. Bio Mater. *4*, 1888–1899.

29. Ronaldson-Bouchard, K., Ma, S.P., Yeager, K., Chen, T., Song, L., Sirabella, D., Morikawa, K., Teles, D., Yazawa, M., and Vunjak-Novakovic, G. (2018). Advanced maturation of human cardiac tissue grown from pluripotent stem cells. Nature *556*, 239–243.

30. Nunes, S.S., Miklas, J.W., Liu, J., Aschar-Sobbi, R., Xiao, Y., Zhang, B., Jiang, J., Massé, S., Gagliardi, M., Hsieh, A., et al. (2013). Biowire: a platform for maturation of human pluripotent stem cell-derived cardiomyocytes. Nat. Methods *10*, 781–787.

31. Herron, T.J., Lee, P., and Jalife, J. (2012). Optical imaging of voltage and calcium in cardiac cells & tissues. Circ. Res. *110*, 609–623.

32. Gintant, G., Kaushik, E.P., Feaster, T., Stoelzle-Feix, S., Kanda, Y., Osada, T., Smith, G., Czysz, K., Kettenhofen, R., Lu, H.R., et al. (2020). Repolarization studies using human stem cell-derived cardiomyocytes: Validation studies and best practice recommendations. Regul. Toxicol. Pharmacol. *117*, 104756.

33. Russell, W.M.S., and Burch, R.L. (1959). The Principles of Humane Experimental Technique (Methuen).

34. Bers, D.M. (2002). Cardiac excitation–contraction coupling. Nature *415*, 198–205.

35. Veerman, C.C., Kosmidis, G., Mummery, C.L., Casini, S., Verkerk, A.O., and Bellin, M. (2015). Immaturity of Human Stem-Cell-Derived Cardiomyocytes in Culture: Fatal Flaw or Soluble Problem? Stem Cell. Dev. *24*, 1035–1052.

36. Garg, P., Garg, V., Shrestha, R., Sanguinetti, M.C., Kamp, T.J., and Wu, J.C. (2018). Human Induced Pluripotent Stem Cell–Derived Cardiomyocytes as Models for Cardiac Channelopathies. Circ. Res. *123*, 224–243.

37. Inoue, H., Yamashita, T., Usui, M., Nozaki, A., and Sugimoto, T. (1991). Antiarrhythmic drugs preferentially produce conduction block at the area of slow conduction in the re-entrant circuit of canine atrial flutter: comparative study of disopyramide, flecainide, and E-4031. Cardiovasc. Res. *25*, 223–229.

38. Doss, M.X., Di Diego, J.M., Goodrow, R.J., Wu, Y., Cordeiro, J.M., Nesterenko, V.V., Barajas-Martínez, H., Hu, D., Urrutia, J., Desai, M., Treat, J.A., Sachinidis, A., and Antzelevitch, C. (2012). Maximum Diastolic Potential of Human Induced Pluripotent Stem Cell-Derived Cardiomyocytes Depends Critically on IKr. PLoS One *7*, e40288.

39. Yu, J., Hu, K., Smuga-Otto, K., Tian, S., Stewart, R., Slukvin, I.I., and Thomson, J.A. (2009). Human induced pluripotent stem cells free of vector and transgene sequences. Science (New York, N.Y.) *324*, 797–801.

40. Reiser, P.J., Portman, M.A., Ning, X.-H., and Schomisch Moravec, C. (2001). Human cardiac myosin heavy chain isoforms in fetal and failing adult atria and ventricles. Am. J. Physiol. Heart Circ. Physiol. *280*, H1814–H1820.

41. Herron, T.J., Vandenboom, R., Fomicheva, E., Mundada, L., Edwards, T., and Metzger, J.M. (2007). Calcium-independent negative inotropy by beta-myosin heavy chain gene transfer in cardiac myocytes. Circ. Res. *100*, 1182–1190.

42. Nielsen, J.B., Thorolfsdottir, R.B., Fritsche, L.G., Zhou, W., Skov, M.W., Graham, S.E., Herron, T.J., McCarthy, S., Schmidt, E.M., Sveinbjornsson, G., Surakka, I., Mathis, M.R., Yamazaki, M., Crawford, R.D., Gabrielsen, M.E., Skogholt, A.H., Holmen, O.L., Lin, M., Wolford, B.N., Dey, R., Dalen, H., Sulem, P., Chung, J.H., Backman, J.D., Arnar, D.O., Thorsteinsdottir, U., Baras, A., O'Dushlaine, C., Holst, A.G., Wen, X., Hornsby, W., Dewey, F.E., Boehnke, M., Kheterpal, S., Mukherjee, B., Lee, S., Kang, H.M., Holm, H., Kitzman, J., Shavit, J.A., Jalife, J., Brummett, C.M., Teslovich, T.M., Carey, D.J., Gudbjartsson, D.F., Stefansson, K., Abecasis, G.R., Hveem, K., and Willer, C.J. (2018). Biobank-driven genomic discovery yields new insight into atrial fibrillation biology. Nat. Genet. *50*, 1234–1239.

43. Fedida, D. (2007). Vernakalant (RSD1235): a novel, atrial-selective antifibrillatory agent. Expet Opin. Invest. Drugs *16*, 519–532.

44. Roy, D., Pratt, C.M., Torp-Pedersen, C., Wyse, D.G., Toft, E., Juul-Moller, S., Nielsen, T., Rasmussen, S.L., Stiell, I.G., Coutu, B., Ip, J.H., Pritchett, E.L.C., and Camm, A.J.; Atrial Arrhythmia Conversion Trial Investigators (2008). Vernakalant Hydrochloride for Rapid Conversion of Atrial Fibrillation. Circulation *117*, 1518–1525.

45. Chen, T.-W., Wardill, T.J., Sun, Y., Pulver, S.R., Renninger, S.L., Baohan, A., Schreiter, E.R., Kerr, R.A., Orger, M.B., Jayaraman, V., Looger, L.L., Svoboda, K., and Kim, D.S. (2013). Ultrasensitive fluorescent proteins for

imaging neuronal activity. Nature *499*, 295–300.

46. Nakai, J., Ohkura, M., and Imoto, K. (2001). A high signal-to-noise Ca(2+) probe composed of a single green fluorescent protein. Nat. Biotechnol. *19*, 137–141.

47. Statzer, C., and Ewald, C.Y. (2020). The extracellular matrix phenome across species. Matrix Biol. *8*, 100039.

48. Sainio, A., and Järveläinen, H. (2020). Extracellular matrix-cell interactions: Focus on therapeutic applications. Cell. Signal. *66*, 109487.

49. Saleem, U., van Meer, B.J., Katili, P.A., Mohd Yusof, N.A.N., Mannhardt, I., Garcia, A.K., Tertoolen, L., de Korte, T., Vlaming, M.L.H., McGlynn, K., Nebel, J., Bahinski, A., Harris, K., Rossman, E., Xu, X., Burton, F.L., Smith, G.L., Clements, P., Mummery, C.L., Eschenhagen, T., Hansen, A., and Denning, C. (2020). Blinded, Multicenter Evaluation of Drug-induced Changes in Contractility Using Human-induced Pluripotent Stem Cell-derived Cardiomyocytes. Toxicol. Sci. *176*, 103–123.

50. Goldfracht, I., Protze, S., Shiti, A., Setter, N., Gruber, A., Shaheen, N., Nartiss, Y., Keller, G., and Gepstein, L. (2020). Generating ring-shaped engineered heart tissues from ventricular and atrial human pluripotent stem cell-derived cardiomyocytes. Nat. Commun. *11*, 75.

51. Wettwer, E., Christ, T., Endig, S., Rozmaritsa, N., Matschke, K., Lynch, J.J., Pourrier, M., Gibson, J.K., Fedida, D., Knaut, M., and Ravens, U. (2013). The new antiarrhythmic drug vernakalant: ex vivo study of human atrial tissue from sinus rhythm and chronic atrial fibrillation. Cardiovasc. Res. *98*, 145–154.

52. Qu, Y., Page, G., Abi-Gerges, N., Miller, P.E., Ghetti, A., and Vargas, H.M. (2017). Action Potential Recording and Pro-arrhythmia Risk Analysis in Human Ventricular Trabeculae. Front. Physiol. *8*, 1109.

53. Jiang, Y., Zhou, Y., Bao, X., Chen, C., Randolph, L.N., Du, J., and Lian, X.L. (2018). An Ultrasensitive Calcium Reporter System via CRISPR-Cas9-Mediated Genome Editing in Human Pluripotent Stem Cells. iScience *9*, 27–35.

54. Acharya, A., Nemade, H., Rajendra Prasad, K., Khan, K., Hescheler, J., Blackburn, N., Hemmersbach, R., Papadopoulos, S., and Sachinidis, A. (2022). Live-Cell Imaging of the Contractile Velocity and Transient Intracellular Ca(2+) Fluctuations in Human Stem Cell-Derived Cardiomyocytes. Cells *11*, 1280.

55. Shinnawi, R., Huber, I., Maizels, L., Shaheen, N., Gepstein, A., Arbel, G., Tijsen, A.J., and Gepstein, L. (2015). Monitoring Human-Induced Pluripotent Stem Cell-Derived Cardiomyocytes with Genetically Encoded Calcium and Voltage Fluorescent Reporters. Stem Cell Rep. *5*, 582–596.

56. Lou, Q., Janardhan, A., and Efimov, I.R. (2012). Remodeling of calcium handling in human heart failure. Adv. Exp. Med. Biol. *740*, 1145–1174.

57. Morgan, J.P., Erny, R.E., Allen, P.D., Grossman, W., and Gwathmey, J.K. (1990). Abnormal intracellular calcium handling, a major cause of systolic and diastolic dysfunction in ventricular myocardium from patients with heart failure. Circulation *81*. Iii21–32.

58. Bedada, F.B., Chan, S.S.K., Metzger, S.K., Zhang, L., Zhang, J., Garry, D.J., Kamp, T.J., Kyba, M., and Metzger, J.M. (2014). Acquisition of a quantitative, stoichiometrically conserved ratiometric marker of maturation status in stem cell-derived cardiac myocytes. Stem Cell Rep. *3*, 594–605.

59. Gu, X., Zhou, F., and Mu, J. (2021). Recent Advances in Maturation of Pluripotent Stem Cell-Derived Cardiomyocytes Promoted by Mechanical Stretch. Med. Sci. Mon. Int. Med. J. Exp. Clin. Res. *27*, e931063.

60. Tzatzalos, E., Abilez, O.J., Shukla, P., and Wu, J.C. (2016). Engineered heart tissues and induced pluripotent stem cells: Macro- and microstructures for disease modeling, drug screening, and translational studies. Adv. Drug Deliv. Rev. *96*, 234–244.

61. Weinberger, F., Mannhardt, I., and Eschenhagen, T. (2017). Engineering Cardiac Muscle Tissue. Circ. Res. *120*, 1487–1500.

62. Chen, X.D., Dusevich, V., Feng, J.Q., Manolagas, S.C., and Jilka, R.L. (2007). Extracellular matrix made by bone marrow cells facilitates expansion of marrow-derived mesenchymal progenitor cells and prevents their differentiation into osteoblasts. J. Bone Miner. Res. *22*, 1943–1956.

63. Marinkovic, M., Block, T.J., Rakian, R., Li, Q., Wang, E., Reilly, M.A., Dean, D.D., and Chen, X.-D. (2016). One size does not fit all: developing a cell-specific niche for in vitro study of cell behavior. Matrix Biol. *52–54*, 426–441.

64. Lian, X., Hsiao, C., Wilson, G., Zhu, K., Hazeltine, L.B., Azarin, S.M., Raval, K.K., Zhang, J., Kamp, T.J., and Palecek, S.P. (2012). Robust cardiomyocyte differentiation from human pluripotent stem cells via temporal modulation of canonical Wnt signaling. Proc. Natl. Acad. Sci. USA *109*, E1848–E1857.

65. Monteiro da Rocha, A., Guerrero-Serna, G., Helms, A., Luzod, C., Mironov, S., Russell, M., Jalife, J., Day, S.M., Smith, G.D., and Herron, T.J. (2016). Deficient cMyBP-C protein expression during cardiomyocyte differentiation underlies human hypertrophic cardiomyopathy cellular phenotypes in disease specific human ES cell derived cardiomyocytes. J. Mol. Cell. Cardiol. *99*, 197–206.

66. Zhang, J., Tao, R., Campbell, K.F., Carvalho, J.L., Ruiz, E.C., Kim, G.C., Schmuck, E.G., Raval, A.N., da Rocha, A.M., Herron, T.J., Jalife, J., Thomson, J.A., and Kamp, T.J. (2019). Functional cardiac fibroblasts derived from human pluripotent stem cells via second heart field progenitors. Nat. Commun. *10*, 2238.

67. Lee, P., Klos, M., Bollensdorff, C., Hou, L., Ewart, P., Kamp, T.J., Zhang, J., Bizy, A., Guerrero-Serna, G., Kohl, P., Jalife, J., and Herron, T.J. (2012). Simultaneous voltage and calcium mapping of genetically purified human induced pluripotent stem cell-derived cardiac myocyte monolayers. Circ. Res. *110*, 1556–1563.

STAR★METHODS

KEY RESOURCES TABLE

REAGENT or RESOURCE	SOURCE	IDENTIFIER
Antibodies		
α-actinin antibody, mouse monoclonal	Sigma	Cat#A7811-2mL; RRID:AB_476766
β-myosin heavy chain antibody, mouse monoclonal, A4.951	Developmental Studies Hybridoma Bank	Cat#A4.951; RRID:AB_528385
Anti-SERCA2a antibody	ThermoFisher	Cat#MA3-919; RRID:AB_325502
Phospho-cTnI antibody	Cell Signaling Technology	Cat#4004S; RRID:AB_2940841
mlc2a antibody	Synaptic Systems	Cat#311 011; RRID:AB_887737
Anti-GFP antibody	Sigma	Cat#G1546; RRID:AB_1079024
Anti-GAPDH antibody	Sigma	Cat#G9545; RRID:AB_796208
Bacterial and virus strains		
AdGCaMP6f	Vector Biolabs	Cat#1910
AdGCaMP6m	Vector Biolabs	Cat#1909
AdGCaMP6s	Vector Biolabs	Cat#1908
Chemicals, peptides, and recombinant proteins		
CalBryte520AM	AAT Bioquest	Cat#21130
JC-1 Dye Mitochondrial Membrane Potential Probe	ThermoFisher	Cat#T3168
Isoproterenol	Sigma	Cat#1351005
E-4031	Sigma	Cat#M5060
Ibutilide	Sigma	Cat#1335610
vernakalant	Sigma	Cat#SML2938
CellTracker Green	ThermoFisher	Cat#C7025
Vandetanib	Cayman Chemical	Cat#14706
Ranolazine	Sigma	Cat#1598744
Domperidone	Sigma	Cat#D122
Critical commercial assays		
PSC-Derived Cardiomyocyte Isolation Kit	Miltenyi Biotec	Cat#130-110-188
Experimental models: Cell lines		
DF19-9-11T.H	WiCell Research Institute	Cat#DF19-9-11T.H
iCell Cardiomyocytes[2]	FUJIFILM/Cellular Dynamics International	Cat#01434
PENN002i-442-1	WiCell Research Institute	Cat#iPS-442-SeV1
WTC-11	Coriell Institute for Medical Research	Cat#GM25256
Software and algorithms		
StemBioSys Optical Electrophysiology Analysis Tool (.oeat)	StemBioSys, Inc./Southwest Research Institute	Cat#OEAT
Other		
CARTOX Optical Mapping Instrument	StemBioSys, Inc/CARTOX	Cat#CARTOX
Cytation5 Imager	Agilent-BioTek	Cat#Cytation5
Incucyte Zoom	Sartorius	Cat#Incucyte

RESOURCE AVAILABILITY

Lead contact

Further information and requests for resources and reagents should be directed to and will be fulfilled by the lead contact, Dr. Todd Joseph Herron (toddherr@umich.edu).

Materials availability

This study produced human cell derived ECM coated cell culture plates in 96 well plate format. High throughput screening plates (96well) coated with this ECM (referred to as MatrixPlus) are available commercially from StemBioSys, Inc.

The high throughput imaging system (CARTOX) is available from CuriBio under the trade name Nautilus. The CARTOX assay is available as a contract research service.

The analysis software (.oeat) is available from StemBioSys, Inc.

Data and code availability

- *Data*
- Original Western Blot images are included in the supplemental data file. Microscopy data reported in this paper will be shared by the lead contact upon request.
- Any additional information required to reanalyze the data reported in this paper is available from the lead contact upon request.
- All data reported in this paper will be shared by the lead contact upon request.
- *Code*
- This paper does not report original code.
- Analysis software will be made available upon request.
- *Requests for reanalysis*
- Any additional information required to reanalyze the data reported in this paper is available upon request from the lead contact.

EXPERIMENTAL MODEL AND STUDY PARTICIPANT DETAILS

Cell lines

hiPSC lines were used to differentiate stem cells to cardiomyocytes. In all cases hiPSCs were maintained as colonies in feeder free conditions in Xeno free stem cell media (iPS Brew, Miltenyi Biotec). hiPSCs were passaged every 5 to 7 days. Cell line authentication was limited to karyotype analysis of hiPSCs to verify cell line sex.

(1) *DF19-9-11T.H hiPSC line was obtained from WiCell Research Institute. This is a male cell line reprogrammed from patient skin fibroblasts; ethnicity is not reported.*

(2) *PENN002i-442-1 hiPSC line was obtained from WiCell Research Institute. This is a female cell line, Caucasian, the patient was 24 years old at the time of collection.*

(3) *WTC-11 hiPSC line (alias: UCSFi001-A) was obtained from Coriell Institute for Medical Research under the identifier GM25256. This is a male cell line, Japanese, the patient was 30 years old at the time of sample collection.*

(4) *iCell Cardiomyocytes*[2] *were obtained as cryopreserved vials of genetically purified human iPSC-CMs from FUJIFILM/Cellular Dynamics International. Cardiomyocytes were thawed and replated in 96 well plates (75,000CMs/well).*

(5) *Use of hiPSCs was done with Institutional Permission of the University of Michigan Human Pluripotent Stem Cell Oversight (HPSCRO) Committee*

METHOD DETAILS

Human extracellular matrix (ECM) production

Decellularized human extracellular matrices were produced using methods adapted from those previously described.[62,63] Amniotic fluid stem cells from an immortalized line originally isolated from amniotic fluid of a full-term birth delivered by planned c-section were seeded onto fibronectin coated cultureware and cultured to confluence in α-Minimum Essential Medium (αMEM), modified without phenol red, supplemented with 2mM stable L-Glutamine, antibiotic-antimycotic, and 15% fetal bovine serum. Half-media

was exchanged after 3 days with cells reaching confluence after 6 days. At confluence, full media was exchanged, and media was supplemented with an additional 50mM ascorbic acid to promote matrix secretion. 72 hours later, the resulting matrices were decellularized using 1% v/v Triton X-100 at room temperature. Decellularized matrices were then washed twice with PBS and once with DI water and then left to airdry. All processes described here are automated using the BioTek MultiFloFX and BioStak4 (BioTek, Winooski, VT). The resulting decellularized and dehydrated matrices are commercially available under the tradename CELLvo™ Matrix Plus by StemBioSys, Inc. The matrices are stored at 4°C and have a shelf-life of 2 years from the date of manufacture. Prior to use, matrices are rehydrated by incubation for 1 hour with PBS at 37C.

Cardiac EP plate reader prototype and analysis software

We designed and fabricated a high resolution cardiac optical mapping plate reader. The plate reader prototype and schematic are shown in Figure S5. We call the Cardiac EP Plate Reader CARTOX™. The CARTOX™ plate reader can record fluorescent changes in all 96 wells of a standard multi well plate in 5 minutes. Other multi-well plates (6wp-384wp) can also be imaged in the cardiac EP plate reader. Multi-well plates were placed on a motorized XY stage with a temperature-controlled stage top incubator maintained at 37°C $\pm$ 0.5°C. Excitation illumination was provided by a custom high-power LED array operating at a wavelength centered at 470nm and fitted with an excitation filter (ET470/40x) and optical diffuser to achieve uniform and homogenous illumination. The fluorescence signals were recorded from a 3.5 x 2.0cm area using a high NA camera lens fitted with a band-pass emission filter (ET525/50M) placed in front of a high speed sCMOS camera sensor (DaVinci2K, SciMeasure). This optical configuration relies on the spontaneous beating characteristic of hiPSC-CM monolayers for data acquisition, future developments will include electrical pacing to match the beat rate for comparisons between plates and wells. The camera was typically operated at frame rates between 100 and 1000fps with recording durations of 10s depending on the experimental needs. All recordings were made using a bespoke acquisition software package developed for the plate reader.

Custom software was developed to enable parallel processing of all well data (Figure S5D). A typical electrophysiological recording of a whole 96 well plate experiment using hiPSC-CMs can be viewed in Video S1. The software has been configured to include automated high content analysis of electrophysiological parameters including beat rate (Hz), action potential duration (APD), action potential triangulation, and conduction velocity. Calcium transients can also be measured with functional readouts including beat rate, amplitude ($\Delta F/F_o$), duration (CaTD), and triangulation. These quantitative values can be observed by generation of heat maps for each multi well plate. An example of a whole plate heat map for spontaneous beat rate is in Figure S6A. The average beat rate in each well is calculated and assigned a color corresponding the frequency (Hz) for that well. Using calcium indicators, a calcium transient amplitude map ($\Delta F/F_o$) can be generated for an entire plate to provide indirect insight on hiPSC-CM monolayer contractility (Figure S6B).

Experimental models: hiPSC-CM cell sources

Commercially available hiPSC-CMs were obtained from Cellular Dynamics International (FUJIFILM, iCell Cardiomyocytes^2 Catalog #: C1016) as cryopreserved vials consisting of >5x10^6 cells per vial. These genetically purified cardiomyocytes were thawed and plated as confluent monolayers, consisting of 75,000 cells per well of each 96 well plate as recently described.[20] Images of iCell Cardiomyocytes^2 were used for demonstration of mature CM structural phenotypes (Figures 1A–1E, S1). These iCell Cardiomyocytes^2 were also utilized for the GCaMP6 analysis (Figures 5, 6, 7, S11, andS12). iCell Cardiomyocytes^2 were maintained in culture for at least seven days prior to phenotype analysis.

hiPSC-CMs were also generated in the laboratory using multiple control hiPSC lines and a well-established cardiac differentiation protocol relying on retinoic acid for atrial CM specification.[17] For chamber specific hiPSC-CM generation two control hiPSC lines were used: 1. The vector free iPS DF19-9-11T.H male cell line,[39] and 2. The vector free iPS PENN002i-442-1 female cell line. Each of these hiPSC lines were obtained from WiCell (Madison, WI). All use of these human iPSC lines were approved by the Human Pluripotent Stem Cell Research Oversight Committee (HPSCRO) of the University of Michigan. In addition, the WTC-11 control hiPSC cell line was utilized to generate non chamber specific cardiomyocytes using small molecule-based approach,[64] these cells were utilized for quantification of the circularity index for CMs plated on Matrigel or MatrixPlus (Figure 1F). On day 20 of the differentiation protocol atrial or ventricular specific hiPSC-CMs were purified using magnetic assisted cell sorting (MACS, Miltenyi Biotec; PSC-Derived

Cardiomyocyte Isolation Kit, human; 130-110-188). The components of this kit are published in a patent application from Miltenyi Biotec (ES2897945T3) and include antibodies to label non-myocytes for depletion followed by direct labeling of cardiomyocytes using SIRPA2α for subsequent enrichment. Purified hiPSC-CMs were plated in Matrigel or MatrixPlus coated 6 well dishes at a density of 35,000 cells/well for determination of circularity index (Figures 1F and S2–S4). In some cases, purified atrial CMs were replated in 96 well plates (75,000 cells per well) to form confluent monolayers, in some cases purified ventricular CMs were replated, and in control cases 50/50 mixture of atrial and ventricular specific CMs were plated for study (Figure 4).

Fluorescent staining and microscopy

hiPSC-CM mitochondria were stained and visualized using JC-1 Dye (Mitochondrial Membrane Potential Probe, ThermoFisher T3168) as described before.[20] JC-1 loaded hiPSC-CMs live cell images were acquired using a Nikon A1R confocal system. 20X images were acquired to enable large fields of view and quantification of many cardiomyocytes JC-1 signal (Figures 1A and 1B). 40X (extra-long working distance) images were also acquired to enable higher magnification of hiPSC-CM mitochondrial distribution and structure (Figures 1A and S1). Red and green fluorescence intensity was quantified per CM using NIS elements software with manual tracing of each cardiomyocyte (20X images, Figure 1B).

hiPSC-CM structure was analyzed using immunofluorescent staining, standard microscopy, and confocal microscopy. For high resolution confocal imaging hiPSC-CM monolayers were plated on plastic coverslips (Thermanox) coated with MatrixPlus human ECM or Matrigel mouse ECM. Matrigel (Corning® Matrigel®, CLS356231) was handled as directed by the manufacturer and as described before.[6,20,27,65,66] After seven days to allow maturation, coverslips of hiPSC-CMs were fixed in paraformaldehyde, blocked in Normal Donkey Serum and myofilament proteins were labeled using primary and corresponding secondary antibodies conjugated to fluorescent probes as done before.[20] Primary antibody directed against α-actinin was used to examine structural phenotypes of immature and mature hiPSC-CMs (iCell Cardiomyocytes[2]; Figure 1C). Confocal microscopy was as before (60X oil objective, galvo scanner, Nikon A1R, 1024x1024 pixels).[18,67] Sarcomere length was quantified by measurement of the fluorescence intensity profile over 25μm lines drawn over individual myocytes to determine average spacing between α-actinin peaks using NIS-Elements software (Figures 1C-D). Cytation 5 (Biotek, Agilent) widefield imager was also used for confirmation of the atrial hiPSC-CM structure/function (Videos S3 andS4) and for detection of GCaMP6 calcium transient recordings following AdGCaMP6f, m or s viral transduction (Figures 5A–5F, and S11 andS12). An example of the calcium transient analysis using the Cytation 5 (20fps) is in Video S5. To optically map monolayers of cardiomyocytes treated with the GCaMP6 virus, a Standard Protocol was run on the Cytation 5 machine using the associated Gen5 software run via BioSpa. The Imaging protocol was run on 96 well Greiner flat bottom plates using Well Mode to switch between emission filters and Kinetic Imaging to capture real-time movies of the monolayers. This was done at a 10X PL FL magnification and utilized the GFP 469,525 channel, which detects the fluorescence changes of the GCaMP6 protein indicator on the monolayers. The Data Reduction Protocol included Kinetic Frame Alignment, Statistical Image Analysis, and Kinetic Well Analysis to provide the mean fluorescent intensity of the green fluorescence values. Gen5 then transformed these images into data sets which were analyzed and generated into graphs based on Relative Intensity Units over time. Fluorescence intensity over time was analyzed using Excel and then plotted and statistics were calculated using GraphPad Prizm software.

Cardiac EP plate reader for action potential and calcium transient analysis

Action potentials were recorded using a voltage sensitive dye (VSD; FluoVolt™ Membrane Potential Kit; F10488 ThermoFisher) with GFP like fluorescence excitation and emission spectra. After 7 days of maturation on MatrixPlus ECM monolayers were loaded with VSD as before[6,8,20,27] and transferred to the Cardiac EP Plate Reader (CARTOX™). In each 96 well plate, a 2x4 array of wells was imaged for 10s (100-500fps) with automated stage/plate translation to a new set of 8 wells until all 96 wells were imaged. Data acquisition of images was done using Turbo software operating the DaVinci 2K CMOS camera (SciMeasure, Atlanta GA). Image acquisition triggering and motorized stage driving was done using Micromanager (ImageJ) software. For each 96 well plate a total of 12 separate movie files were stitched together for parallel processing using StemBioSys Optical Electrophysiology Analysis Tool (* *.oeat files) Software. The OEAT files were used for automated calculation of spontaneous beat rate, action potential duration (APD30, 50, 80, 90), action potential triangulation (APD90-APD30/APD90), and conduction velocity.

Calcium transients were recorded using CalBryte520AM (5μM), a calcium sensitive probe that fluoresces green upon calcium binding using the Cardiac EP plate reader. In other experiments calcium flux was quantified using GCaMP6. In these experiments using GECI, recombinant adenovirus was applied to hiPSC-CM monolayers and beginning on day 3 after virus transduction GCaMP6 calcium flux could be recorded using the Cardiac EP plate reader. The imaging routine was identical for calcium transient recordings as for VSDs listed above. Analysis for calcium transients was like action potentials but using the calcium analysis mode in the .oeat files. A typical whole plate recording of spontaneous calcium transients in atrial specific hiPSC-CM monolayers can be viewed in Video S1. CalBryte520AM was used for acute experiments and acute exposure of drugs, GCaMP6 recordings were made daily from day 3 after viral gene delivery up to day 8 after gene delivery.

GCaMP6fast, medium or slow variant acute gene transfer

GCaMP6 is a calcium sensitive green fluorescent protein used to monitor intracellular calcium flux. Here we tested the effect of three different GCaMP6 genetic variants called GCaMP6fast, medium or slow. The kinetic designation indicates the rate of calcium binding and unbinding to the GCaMP6 protein probe. Recombinant adenoviruses were obtained from Vector Biolabs (Malvern, PA: AdGCaMP6f, cat#1910; AdGCaMP6m, cat#1909; AdGCaMP6s, cat#1908). All viruses' backbone is adenovirus-type 5 (dE1/E3) and GCaMP6 variant expression was driven by the CMV (cytomegalovirus) promoter. Viral titer is identical for each virus ($1x10^{10}$ PFU/mL), stocks were aliquoted for single use to avoid freeze/thaw cycles and stored in DMEM w/2% SA &2.5% glycerol at -80°C. Each virus was used at a load of 5moi (multiplicity of infection) and applied to hiPSC-CM monolayers (CDI, iCell Cardiomyocytes[2]) in a volume of 100μL per well of 96 well plate overnight. Virus was added to monolayers 4 days after thaw and plating of cryopreserved CMs. Efficiency of gene transfer in hiPSC-CM monolayers was calculated using fluorescent images confluence relative to total phase contrast confluence and found to be ≥80% for all viruses (Figure S12B). Calcium transients could be observed using an inverted microscope imager (Cytation 5) one day post gene transfer and we repeated measurements of the same plate over eight days (Figures 5 and S11). On day 3 after gene transfer calcium transients could be imaged using the Cardiac EP plate reader and we repeated measurements on this device daily until day 7 after the acute gene transfer of GCaMP6 variants (Figures 6G–6W). GCaMP6 variant protein expression was determined to be equal on Day 8 after gene delivery by Western Blot analysis, probing for GFP expression (Figures S11D and S11E). Also, SERCA2a calcium pump expression was found to be similar in hiPSC-CMs regardless of the GCaMP6 variant expression (Figures S11F and S11G).

Western blot analysis

Protein expression was analyzed using Western Blot approaches as described before.[8,18,20] Following optical mapping experiments hiPSC-CM monolayers were solubilized using Laemmli Sample Buffer (50μL per well, BioRad, #161-0737). The solubilized protein of 2 wells were collected in a single tube for subsequent gel electrophoresis (NuPage gels, 4-12%) and transfer to nitrocellulose membranes (InVitrogen Power Blotter). Following transfer total protein staining was done using PonceauS to confirm protein transfer. After transfer, the protein remaining in the acrylamide gel was stained using Coomassie blue dye (BioRad, 161-0803) for total protein normalization. Next, membranes were blocked using 5% milk (in phosphate buffered saline, PBS), washed (PBS+0.001% Tween 20), incubated with primary antibody (1/1000 diluted in PBS-Tween-5% milk), washed again, incubated with the appropriate immunoglobulin matched secondary antibody conjugated to horseradish peroxidase (HRP) for detection using enhanced chemiluminescence (ECL) reagent. Primary antibodies used include mouse anti β-myosin heavy chain (A4.951, Developmental Studies Hybridoma Bank), mouse anti-MLC-2a (Synaptic Systems), mouse anti-GFP (Millipore Sigma), mouse anti-SERCA2a (Thermo Fisher, MA3-919), and rabbit anti phospho-cTnI (Cell Signaling Technology, 4004S). Membranes were imaged using a BioRad Gel Doc system and analyzed using ImageJ Gel Analysis tool.

Drug/medication testing

Ranolazine, Domperidone, Ibutilide and Vandetanib were obtained and used as recently described and informed by the FDA validation study.[5] Dosing was based on clinical data for the Cmax of each drug. Each drug compound was diluted using DMSO and stored in -20°C as 1000X stock solutions. E-4031 was solubilized in DMSO (10mM), stored at -20°C and diluted to 0.50μM in HBSS for exposure to monolayers. Vernakalant was dissolved in DMSO and stored at -20°C in 10mM stock solution. On the day of experimentation 1X drug concentrations were made by diluting stock in Hanks Balanced Salt Solution (HBSS, +Ca).

Following baseline recordings, drug was added to each well (100μL), allowed to equilibrate and warm for 30 min and then another recording was made to determine medication effects. The 30min incubation period was carried out in the tissue culture incubator. Isoproterenol (ISO) was solubilized in DMSO (10mM, stock solution) and diluted to 0.10μM for acute application to hiPSC-CM monolayers or 0.20 μM for daily pulsing experiments. ISO effects were recorded 5 min following exposure. Recordings using GECI were made in cell culture media (RPMI, No Phenol Red) with direct transfer from the tissue culture incubator to the CARTOX machine for rapid recording with subsequent return to the tissue culture incubator.

QUANTIFICATION AND STATISTICAL ANALYSIS

Statistical analysis was performed using GraphPad Prizm 9. The specific statistical tests used, details of technical replicates and summary of mean data ± standard deviation are included in the legend of each figure. In summary, instances comparing two groups utilized paired t-tests or unpaired t-tests where appropriate with $P<0.05$ indicating significance. Instances comparing three or more groups of data utilized One way ANOVA analysis with post hoc analysis, Tukey's multiple comparisons test was used. The P values are indicated in each figure or figure legend.